

REVIEW

Thermal protein unfolding by differential scanning calorimetry and circular dichroism spectroscopy Two-state model *versus* sequential unfolding

Joachim Seelig^{1*} and Hans-Joachim Schönfeld²

¹Division of Biophysical Chemistry, Biozentrum, University of Basel, Klingelbergstrasse 50/70, CH-4056 Basel, Switzerland

²Schönfeld – Protein Science Consulting, Marienmattenweg 7, DE-79115 Freiburg, Germany

Quarterly Reviews of Biophysics (2016), 49, e9, page 1 of 24 doi:10.1017/S0033583516000044

Abstract. Thermally-induced protein unfolding is commonly described with the two-state model. This model assumes only two types of protein molecules in solution, the native (N) and the denatured, unfolded (U) protein. In reality, protein unfolding is a multistep process, even if intermediate states are only sparsely populated. As an alternative approach we explore the Zimm–Bragg theory, originally developed for the α -helix-to-random coil transition of synthetic polypeptides. The theory includes intermediate structures with concentrations determined by the cooperativity of the unfolding reaction. We illustrate the differences between the two-state model and the Zimm–Bragg theory with measurements of apolipoprotein A-1 and lysozyme by differential scanning calorimetry (DSC) and CD spectroscopy. Nine further protein examples are taken from the literature. The Zimm–Bragg theory provides a perfect fit of the calorimetric unfolding transitions for all proteins investigated. In contrast, the transition curves and enthalpies predicted by the two-state model differ considerably from the experimental results. Apolipoprotein A-1 is ~50% α -helical at ambient temperature and its unfolding follows the classical α -helix-to-random coil equilibrium. The unfolding of proteins with little α -helix content, such as lysozyme, can also be analyzed with the Zimm–Bragg theory by introducing the concept of ‘folded’ and ‘unfolded’ peptide units assuming an average unfolding enthalpy per peptide unit. DSC is the method of choice to measure the unfolding enthalpy, ΔH_{exp}^0 , but CD spectroscopy in combination with the two-state model is often used to deduce the unfolding enthalpy. This can lead to erroneous result. Not only are different enthalpies required to describe the CD and DSC transition curves but these values deviate distinctly from the experimental result. In contrast, the Zimm–Bragg theory predicts the DSC and CD unfolding transitions with the same set of parameters.

1. Introduction 2

2. Two-state model *versus* sequential protein unfolding 3

2.1. Temperature course of heat capacity and enthalpy 3

2.2. Two-state model 4

2.3. Zimm–Bragg theory. Sequential protein unfolding 5

2.4. Energetics of ‘folded’ peptide units in globular proteins 6

3. Protein unfolding measured with CD spectroscopy 7

3.1. CD experiments with human Apo A-1. Unfolding of an α -helical protein 7

* Author for correspondence: Joachim Seelig, Division of Biophysical Chemistry, Biozentrum, University of Basel, Klingelbergstrasse 50/70, CH-4056 Basel, Switzerland. Tel.: +41-61-267 2190; Fax: +41-61-267 2189; Email: joachim.seelig@unibas.ch



3.2. Two-state model applied to Apo A-1 unfolding	9
3.3. Zimm–Bragg theory applied to Apo A-1 unfolding	9
3.4. Lysozyme unfolding. A globular protein with α/β -structure	10
3.5. Sloping baselines in CD spectroscopy	11
4. Thermal unfolding measured with DSC	11
4.1. Calorimetry of Apo A-1	11
4.2. Calorimetry of lysozyme	12
4.3. A 50-amino acid peptide	13
4.4. Proteins selected from the literature	14
5. Cooperative unfolding and two-state model applied to DSC and CD spectroscopy	17
5.1. The total heat of unfolding ΔH_{exp}^0	17
5.2. Equivalence of DSC and CD spectroscopy unfolding transitions?	17
6. Zimm–Bragg theory applied to globular proteins	20
6.1. Zimm–Bragg theory. An excellent thermodynamic approach to protein unfolding	20
6.2. The free energy change upon thermal and chemical denaturation	21
7. Conclusions	21
Supplementary material	21
Acknowledgements	22
References	22

1. Introduction

Proteins can fold spontaneously into their native conformations. The folding/unfolding transition is a highly cooperative process characterised by the presence of no or very few thermodynamically stable intermediate states. ‘Small globular proteins of molecular weight less than 20 kDa usually undergo folding/unfolding transitions in which the only two conformations that become significantly populated at any point during the transition are the folded and unfolded states. The entire protein essentially behaves as a single cooperative unit’ (Privalov *et al.* 1989). However, even when intermediate states are not significantly populated, the folding/unfolding transition is a sequential process, as, for example, the α -helix-to-coil transition. The cooperative interaction of protein domains may then constitute a next higher level of cooperativity (Freire & Murphy, 1991).

Thermal unfolding of a protein requires heat and leads to a reorganization of the protein structure. Different physical-chemical methods are employed to quantify the unfolding transition. Differential scanning calorimetry (DSC) measures the heat consumed and constitutes the reference method for the thermodynamic analysis. Spectroscopic methods, in particular circular dichroism (CD) spectroscopy, provide structural data.

As an example, Fig. 1 shows DSC and CD spectroscopy unfolding transitions of apolipoprotein A-1 (Apo A-1). Identical protein solutions were used in the two experiments. The heat uptake is reflected in an increase of the molar heat capacity, C_p . The area under the $C_p(T)$ versus temperature curve yields the total unfolding enthalpy, ΔH_{exp}^0 , which comprises the enthalpy of the conformational change and the enthalpy change brought about by the increased heat capacity of the unfolded protein.

The mean residue ellipticity at 222 nm, $\epsilon_{222\text{nm}}$, is shown in parallel and is a quantitative measure of the α -helix content of Apo A-1. The structural change is tightly linked to the thermodynamic equilibrium, but thermodynamic information can be derived only indirectly by applying an unfolding model. In contrast, DSC is a model-free thermodynamic method.

The two-state model is commonly applied in spectroscopic studies, be it for heat denaturation or for isothermal denaturation with chemical reagents. The model recognizes just two conformations, the native N and the unfolded U conformation (for reviews see references (Bolen & Yang, 2000; Konermann, 2012; Zhou *et al.* 1999)). The two-state model simplifies, however, the reaction pathway as the unfolding of a protein is truly a sequential process illustrated, for example, by the zipper-like opening of an α -helical domain. A sequential cooperative model such as described by the Zimm–Bragg theory can be expected to provide a more realistic physical insight (Zimm & Bragg, 1959). The present review addresses two questions. (i) We compare DSC and CD spectroscopy with respect to the thermodynamic information derived. (ii) We compare two-state unfolding with sequential unfolding. Which model provides a consistent description of both the calorimetric and spectroscopic

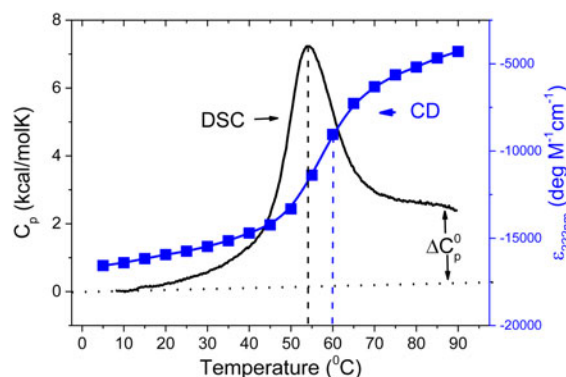


Fig. 1. Differential scanning calorimetry and CD spectroscopy – two methods to study protein unfolding. Thermal unfolding of apolipoprotein A-1 (100 μM in PBS buffer).

experiments? Can the Zimm–Bragg theory, originally developed for the α -helix-to-coil transition, be extended to globular proteins with little α -helix content?

In the following, the basic features of the two-state model and the Zimm–Bragg theory are introduced and applied to the analysis of CD spectroscopy and DSC unfolding experiments. Human Apo A-1, $\sim 50\%$ α -helical protein, and egg white lysozyme, a globular protein with little α -helical content, are chosen to represent two proteins of opposite character. CD-measured unfolding transitions of both proteins are quantified by spectral simulation and analysed with the two models. Identical protein solutions are also measured with DSC and evaluated accordingly. A quantitative thermodynamic comparison of (i) CD spectroscopy *versus* DSC and (ii) two-state model *versus* Zimm–Bragg theory is thus possible.

In addition, literature data are analysed with both the two-state model and the Zimm–Bragg theory. A 50-amino acid peptide and 6 proteins with rather well-documented DSC and CD transition curves were selected. In addition, several high-quality DSC scans of proteins for which no spectroscopic data are available, were also analysed with both models.

2. Two-state model *versus* sequential protein unfolding

The predominant measuring parameter in protein unfolding experiments is the fraction of unfolded protein, $\Theta_U(T)$. It is commonly deduced from changes in the fluorescence intensity or ellipticity and is tightly linked to the thermodynamics of the unfolding reaction. In DSC the physical readout is the heat capacity $C_{p,NU}(T)$ yielding simultaneously the enthalpy of unfolding $\Delta H_{cal}(T)$. The latter is given by the area underneath the $C_{p,NU}(T)$ *versus* T curve and can be evaluated without the need for a specific unfolding model. In contrast, spectroscopic experiments provide thermodynamic information only by applying an appropriate folding model. Thermodynamic results derived from spectroscopic data are thus indirect and model-dependent.

2.1 Temperature course of heat capacity and enthalpy

Protein unfolding is not a true physical phase transition where the total heat is absorbed at a fixed temperature. Instead, the heat of unfolding, $\Delta H_{cal}(T)$, is consumed over an extended temperature range $\Delta T = T_{end} - T_{ini}$ and its temperature-dependence follows the change in heat capacity, $C_{p,NU}(T)$

$$\Delta H_{cal}(T) = \int_{T_{ini}}^T C_{p,NU}(T) dT \quad (1)$$

$\Delta H_{cal}(T)$ comprises contributions from (i) the conformational enthalpy ΔH_{NU}^0 , associated with the conformational change proper, and (ii) the increased heat capacity of the unfolded protein given by

$$\Delta C_{p,NU}^0 = C_{p,U}^0 - C_{p,N}^0 \quad (2)$$

The heat capacity of the unfolded protein, $C_{p,U}^0$, is larger than that of the native protein, $C_{p,N}^0$, because additional water molecules bind to the open structure (Myers *et al.* 1995; Privalov & Dragan, 2007). $\Delta C_{p,NU}^0$ is detected only with DSC but not with CD spectroscopy (unless the unfolding transition at low temperature ('cold denaturation') can also be measured (Nicholson & Scholtz, 1996)). The increase in heat capacity makes an important contribution to the *total* unfolding enthalpy (Privalov & Dragan, 2007). Consequently, the conformational enthalpy ΔH_{NU}^0 alone is insufficient to describe the thermodynamics of the



unfolding process and must be complemented by a temperature-dependent heat capacity term

$$\Delta H_{\text{NU}}(T) = \Delta H_{\text{NU}}^0 + \Delta C_{\text{p,NU}}^0(T - T_0) \quad (3)$$

For reasons given below the midpoint of the conformational transition is chosen as reference temperature T_0 .

The theoretical expression for the experimentally accessible enthalpy $\Delta H_{\text{exp}}(T)$ is obtained by multiplying $\Delta H_{\text{NU}}(T)$ (Eq. (3)) with the fraction of unfolded protein, $\Theta_{\text{U}}(T)$.

$$\Delta H(T) = \Delta H_{\text{NU}}(T)\Theta_{\text{U}}(T) = \left[\Delta H_{\text{NU}}^0 + \Delta C_{\text{p,NU}}^0(T - T_0) \right] \Theta_{\text{U}}(T). \quad (4)$$

In a perfect simulation $\Delta H(T)$ is identical with the experimental $H_{\text{exp}}(T)$.

The predicted heat capacity is the derivative of $H(T)$ with respect to temperature

$$C_{\text{p,NU}}(T) = \Delta H_{\text{NU}}(T) \frac{d\Theta_{\text{U}}(T)}{dT} + \Delta C_{\text{p,NU}}^0 \Theta_{\text{U}}(T) \quad (5)$$

The first term on the right side of Eq. (5) is the specific contribution of the conformational change, the second term that of the increased heat capacity. The enthalpy change caused by $\Delta C_{\text{p,NU}}^0$ alone is given by

$$\Delta H_{\text{Cp,NU}}^0 = \int_{T_{\text{ini}}}^{T_{\text{end}}} \Delta C_{\text{p,NU}}^0 \Theta_{\text{U}}(T) dT \quad (6)$$

$\Theta_{\text{U}}(T)$ must be calculated with either the two-state model or the Zimm–Bragg theory (see Sections 2.2 and 2.3).

Knowledge of $\Delta H_{\text{NU}}(T)$ leads to further thermodynamic parameters. The protein unfolding equilibrium is determined by the change in free energy, $\Delta G_{\text{NU}}(T)$.

$$\Delta G_{\text{NU}}(T) = \Delta H_{\text{NU}}(T) - T\Delta S_{\text{NU}}(T) \quad (7)$$

Taking into account the change in heat capacity, $\Delta C_{\text{p,NU}}^0$, the unfolding entropy $\Delta S_{\text{NU}}(T)$ is given by

$$\Delta S_{\text{NU}}(T) = \Delta S_{\text{NU}}^0 + \Delta C_{\text{p,NU}}^0 \ln \frac{T}{T_0} \quad (8)$$

ΔS_{NU}^0 is not known independently. However, at the midpoint T_0 of the phase transition, equal fractions of native and unfolded protein exist in the solution, the equilibrium constant is $K_{\text{NU}}(T_0) = \Theta_{\text{U}}(T_0)/(1 - \Theta_{\text{U}}(T_0)) = 1$, and the free energy is $\Delta G_{\text{NU}}(T_0) = 0$, yielding

$$\Delta H_{\text{NU}}^0 = T_0 \Delta S_{\text{NU}}^0 \quad (9)$$

The Gibbs free energy is thus simplified to

$$\Delta G_{\text{NU}}(T) = H_{\text{NU}}^0 \left(1 - \frac{T}{T_0} \right) + \Delta C_{\text{p,NU}}^0(T - T_0) - T \Delta C_{\text{p,NU}}^0 \ln \frac{T}{T_0} \quad (10)$$

with ΔH_{NU}^0 and $\Delta C_{\text{p,NU}}^0$ as the only free parameters. In spectroscopic experiments $\Delta C_{\text{p,NU}}^0$ cannot be measured. A truncated formula is used as $\Delta C_{\text{p,NU}}^0 = 0$

$$\Delta G_{\text{NU}}(T) = H_{\text{NU}}^0 \left(1 - \frac{T}{T_0} \right) \quad (11)$$

2.2 Two-state model

The quantitative analysis of protein unfolding is almost exclusively based on the two-state model (Bolen & Yang, 2000; Konermann, 2012; Zhou *et al.* 1999). It assumes that a protein in solution adopts only two conformational states, the native (N) and the unfolded (U) state. The equilibrium $\text{N} \rightleftharpoons \text{U}$ is described with a temperature-dependent equilibrium constant $K_{\text{NU}}(T)$.

$$K_{\text{NU}}(T) = \frac{[\text{U}]}{[\text{N}]} = \frac{\Theta_{\text{U}}(T)}{1 - \Theta_{\text{U}}(T)} = \frac{1 - \Theta_{\text{N}}(T)}{\Theta_{\text{N}}(T)} \quad (12)$$

$[\text{N}]$ and $[\text{U}]$ are the equilibrium concentrations of the native and the unfolded protein, respectively, and $\Theta_{\text{U}}(T)$ and $\Theta_{\text{N}}(T)$ are



the fractions of unfolded and native protein, respectively.

$$\Theta_U(T) = \frac{[U]}{[U] + [N]} = \frac{K_{NU}(T)}{1 + K_{NU}(T)} \quad (13)$$

With this definition a stable native protein is characterised by a *small* equilibrium constant. $K_{NU}(T)$ is related to the Gibbs free energy according to

$$\Delta G_{NU}(T) = -RT \ln K_{NU}(T) \quad (14)$$

The temperature dependence of $K_{NU}(T)$ is thus

$$K_{NU}(T) = e^{-\Delta G_{NU}(T)/RT} \quad (15)$$

where $\Delta G_{NU}(T)$ is given by Eqs. (10) or (11). Eq. (15) allows the calculation of the fraction of unfolded protein, $\Theta_U(T)$, over the whole temperature range.

An approximation of Eq. (15) is the van't Hoff equation, which is commonly used in the evaluation of spectroscopic experiments.

$$\ln \frac{K_2}{K_1} = -\frac{\Delta H_{NU}^0}{R} \left(\frac{1}{T_2} - \frac{1}{T_1} \right) \quad (16)$$

It is based on Eq. (11) and assumes that the unfolding enthalpy is independent of temperature. ($\Delta C_{p,NU}^0 = 0$). A plot of $\ln K(T)$ versus the reciprocal absolute temperature, $1/T$, yields a straight line with slope $-\Delta H_{NU}^0/R$.

The total free energy change associated with the unfolding reaction is a physical property of general interest. If K_{ini} at temperature T_{ini} and K_{end} at temperature T_{end} denote beginning and end of the conformational change, then the free energy change is given by

$$\Delta G_{NU}^0 = RT \ln \left(\frac{K_{end}}{K_{ini}} \right) \quad (17)$$

2.3 Zimm–Bragg theory. Sequential protein unfolding

The advantage of the two-state model is its simplicity. On the other hand, it ignores or even contradicts the molecular mechanism of unfolding. A physically more realistic model for a sequential process is provided by the Zimm–Bragg theory (Zimm & Bragg, 1959), which successfully describes the α -helix-to-coil transition of synthetic polypeptides, but is not commonly applied to protein unfolding. A review on recent advances in helix-coil theory is available (Doig, 2002).

The two-state model requires the total unfolding enthalpy, $\Delta H_{NU}(T)$, as the input parameter. In contrast, the sequential Zimm–Bragg theory is based on the much smaller enthalpy ' h ' of the elementary step. The change of a *single* peptide unit from α -helix ('folded') to coil ('unfolded') conformation is the basic two-state equilibrium. It nevertheless involves several peptide units and leads to the cooperative reorganization of all torsion angles between peptide units i and $i + 3$.

Typically, a protein solution will contain a mixture of molecules, all with different helix contents, ranging from all helix to all coil. 'In order to interpret experiments on helical peptides and make theoretical predictions on helices, it is therefore essential to use a helix-coil theory that considers every possible location of the helix within a sequence' (Doig, 2002). In the following, we will use the Zimm–Bragg formalism in its simplest form (Davidson, 1962).

In this model the fractions of helix and random coil amino acid residues are determined by three parameters: the nucleation parameter σ , the enthalpy of helix formation h , and the chain length N .

The nucleation parameter σ defines the cooperativity of the folding/unfolding equilibrium. The smaller σ , the steeper is the cooperative conformational transition. σ is assumed to be temperature-independent and typical values are $\sigma \sim 10^{-3}$ – 10^{-6} . The nucleation parameter σ is strictly defined for homopolymers. If the peptide chain contains different amino acids, σ is an average value over the different amino acids involved.

The enthalpy h determines the growth parameter, $s(T)$

$$s(T) = e^{-(h/R)(1/T) - (1/T_\infty)} \quad (18)$$



$s(T)$ is the equilibrium constant for the addition of an α -helical peptide unit to an existing α -helix. The equilibrium constant for the formation of a helical peptide unit within a stretch of random coil peptide units is smaller by the factor σ and is $\sigma s(T)$.

The characteristic temperature, T_∞ , is identical with the midpoint of the unfolding transition for a sufficiently long peptide chain with $N \gg \sigma^{-1/2}$.

The mathematical formalism of the Zimm–Bragg theory can be summarised as follows. A polypeptide chain of N peptide units adopts a maximum of 2^N conformations as each segment can be either coil (c) or helix (h). If a polypeptide chain of length i ends on c or h , the addition of a further segment at position $i + 1$ leads to the combinations cc , hc , ch and hh . The conditional probabilities of occurrence are combined in the matrix M (Davidson, 1962)

$$M = \begin{pmatrix} 1 & \sigma s \\ 1 & s \end{pmatrix} \quad (19)$$

where s is given by Eq. (18). M is used to calculate the partition function Z

$$Z(\sigma, s, N) = \begin{pmatrix} 1 & 0 \\ 1 & 0 \end{pmatrix} \begin{pmatrix} 1 & \sigma s \\ 1 & s \end{pmatrix}^N \begin{pmatrix} 1 \\ 1 \end{pmatrix} \quad (20)$$

from which the helix fraction can be calculated

$$\Theta_{\text{helix}}(T) = \frac{s}{N} \frac{d(\ln Z(\sigma, s, N))}{dT} \left(\frac{ds}{dT} \right)^{-1} \quad (21)$$

In combination with Eqs. (4) and (5), Eq. (21) predicts the thermodynamics of sequential unfolding.

The Gibbs free energy of the unfolding transition, ΔG_{NU}^0 , is determined by the growth parameter $s(T)$. With T_{ini} and T_{end} denoting the beginning and the end of the unfolding transition, respectively, the total free energy change of N peptide units is given by

$$\Delta G_{\text{NU}}^0 = -NRT_0 \ln \frac{s(T_{\text{end}})}{s(T_{\text{ini}})} \quad (22)$$

The Zimm–Bragg theory allows the calculation of probabilities of specific conformations. Of particular interest is n_σ , the number of nuclei within the linear sequence. It can be calculated according to

$$n_\sigma(T) = \sigma \frac{d \ln Z(\sigma, s, N)}{d\sigma} \quad (23)$$

2.4 Energetics of ‘folded’ peptide units in globular proteins

α -Helices and β -sheets are the dominant structural elements in proteins. It is usually assumed that the formation of these structures is driven by the formation of peptide hydrogen bonds (Privalov & Makhatadze, 1993). This predicts an only marginal stability of helices in water because hydrogen bonds between peptide units and water appear to be more favorable. Unexpectedly and in contrast to this classical view, short alanine-based peptides showed stable α -helix formation in H_2O (Marqusee *et al.* 1989). It was concluded that individual alanine residues had a high helix-forming potential and that hydrophobic interactions played an important role in stabilising isolated α -helices (Marqusee *et al.* 1989). Helix formation was induced by the gain in free energy upon burial of hydrophobic groups from water in adopting the helical conformation. It was concluded that ‘hydrophobic interaction may be an important determinant of α -helix stability’ (Marqusee *et al.* 1989). Earlier literature supporting this finding is listed in the same reference.

Free energy calculations using the CHARMM potential function and accounting for solvation effects with various continuum solvation models also argue against a dominant energetic role of hydrogen bonds for α -helix and β -sheet stability (Yang & Honig, 1995a, b). Hydrogen bond formation was found to contribute little to α -helix stability because the internal hydrogen bonding energy is largely canceled by the large free energy cost associated with removing polar groups from water. The major driving force favoring helix formation was associated with enhanced van der Waals interactions in the close-packed helix conformation and the hydrophobic effect (Yang & Honig, 1995b).

Corresponding calculations were made for β -sheets. ‘In parallel with our study of α -helices we find that van der Waals and hydrophobic interactions are the primary factor stabilizing polyalanine β -sheets, while electrostatic interactions including hydrogen bonding are found to be destabilizing. However, in contrast to helices, the net change in conformational free energy



involving only backbone–backbone interactions (including β -carbons) is not sufficient to overcome the loss in configurational entropy that accompanies sheet formation. Rather we suggest that cross-strand non-polar side chain – side chain interactions are essential for sheet formation, explaining why large non-polar amino acids have the greatest sheet forming propensities' (Yang & Honig, 1995a).

It follows from these experimental and theoretical studies that (i) specific hydrogen bonds are not the dominant energetic factors in secondary structures of proteins, and (ii) the energetics is determined by van-der-Waals and hydrophobic interactions in the folded protein. A decrease in non-polar accessible surface area favors helix formation.

These theoretical and experimental results suggest a conceptual extension of the Zimm–Bragg theory for globular proteins. The sequential unfolding is considered to be a change from 'folded' to 'unfolded' peptide units. We postulate an average energetic difference (enthalpy h ; free energy, g) between 'folded' and 'unfolded' peptide units, identical for all residues. Moreover, the free energy of a peptide unit is not connected to the formation of specific hydrogen bond but requires simply the well-defined burial of a 'folded' residue in the native protein structure.

At the present stage it is helpful to summarise the energetic parameters obtained for α -helix and β -sheet formation as they serve as energetic markers for the generalised concept. A large number of calorimetric studies has shown that the enthalpy of α -helix formation is $h_{\text{helix}} \sim -1.1 \text{ kcal mol}^{-1}$ (Chou & Scheraga, 1971; Rialdi & Hermans, 1966; Scholtz *et al.* 1991a, b). The h -parameter is smaller if α -helix formation occurs in a hydrophobic environment. A value of $h_{\text{helix}} = -0.7 \text{ kcal mol}^{-1}$ was reported for α -helix formation in tri-fluoroethanol-water mixtures (Luo & Baldwin, 1997).

For the membrane-induced α -helix formation of the antimicrobial peptide magainin 2 the enthalpy change was $h_{\text{helix}} \sim -0.7 \text{ kcal mol}^{-1}$ per residue and the free energy change $g_{\text{helix}} \sim -0.14 \text{ kcal mol}^{-1}$ per residue (Wieprecht *et al.* 1999). The corresponding parameters of rat mitochondrial rhodanese pre-sequence were $h_{\text{helix}} \sim -0.5$ to $-0.6 \text{ kcal mol}^{-1} \text{ residue}^{-1}$ and $g_{\text{helix}} \sim -0.2 \text{ kcal mol}^{-1}$ (Wieprecht *et al.* 2000). For two other amphipathic peptides measured under different experimental conditions a value of $g_{\text{helix}} \sim -0.25 \text{ kcal mol}^{-1}$ has been reported (Fernandez-Vidall *et al.* 2007; Li *et al.* 2003).

Less information is available on the thermodynamic and kinetic parameters of the random coil \rightleftharpoons β -structure transition. The contribution of the β -sheet formation to the overall folding process was determined with analogues of the KIGAKI repeat where two adjacent amino acids were replaced by their D-enantiomers (Meier & Seelig, 2007). The thermodynamic parameters were $h_{\beta} = -0.23 \text{ kcal mol}^{-1}$ per residue and a free energy change of $g_{\beta} = -0.15 \text{ kcal mol}^{-1}$ residue (Meier & Seelig, 2007).

In contrast to α -helix formation, the thermodynamic parameters of β -sheet formation depend on the size of the β -sheet segment (Meier & Seelig, 2008). The folding reaction for peptides with $n \geq 12$ is characterized by $g_{\beta} \sim -0.15 \text{ kcal mol}^{-1}$ per amino acid residue and $h_{\beta} \sim -0.2$ to $-0.6 \text{ kcal mol}^{-1}$ per residue. For a short chain with $n = 12$, β -sheet formation is unfavorable with $g_{\beta} \sim +0.08 \text{ kcal mol}^{-1}$ per residue (Meier & Seelig, 2008).

The free energy of a peptide unit can also be estimated from the growth parameter s . For the short alanine-based peptide Ac-(AAAAK)₃A-NH₂, which has a substantial helix content at low temperature the s -parameter is $s = 1.58$ and the free energy $g_{\text{helix}} = -0.16 \text{ kcal mol}^{-1}$ for $\Theta_{\text{helix}} = 0.36$ at 20 °C (fit parameters: $\sigma = 8 \times 10^{-4}$, $h = -1.4 \text{ kcal mol}^{-1}$) (Marqusee *et al.* 1989; Yang & Honig, 1995b).

3. Protein unfolding measured with CD spectroscopy

3.1 CD experiments with human Apo A-1. Unfolding of an α -helical protein

Human Apo A-1 is a 28.2 kDa protein (243 aa) involved in the reverse transport and metabolism of cholesterol. It has been widely investigated for its role in reducing cardiovascular risks. CD spectroscopy reports an α -helix content of $\sim 50\%$ for Apo A-1 in solution (at room temperature) (Arnulphi *et al.* 2004; Gursky & Atkinson, 1996; Saito *et al.* 2003b, 2004; Schulthess *et al.* 2015; Suurkuusk & Hallen, 1999; Zehender *et al.* 2012). The 2.2-Å crystal structure of a truncated $\Delta(185\text{--}243)$ Apo A-1 reveals long stretches of α -helix ($\sim 80\%$ helix) (Mei & Atkinson, 2011). When heated, Apo A-1 displays an unfolding transition centered at about 55 °C, which is fully reversible both in CD and DSC experiments. The thermal unfolding of Apo A-1 is a true chemical equilibrium if the molecule is not heated above 90 °C.

Figure 2a shows CD spectra of recombinant Apo A-1 (245 aa, 2 additional N-terminal glycine residues) as a function of temperature. The two bold lines define the spectra recorded at the lowest (5 °C, black line) and highest temperature (90 °C, olive line), i.e. the spectra with the highest and lowest α -helix content, respectively. An apparent isodichroic point is observed at 203 nm. Increasing the resolution around 203 nm reveals however small deviations from a single cross-over point.

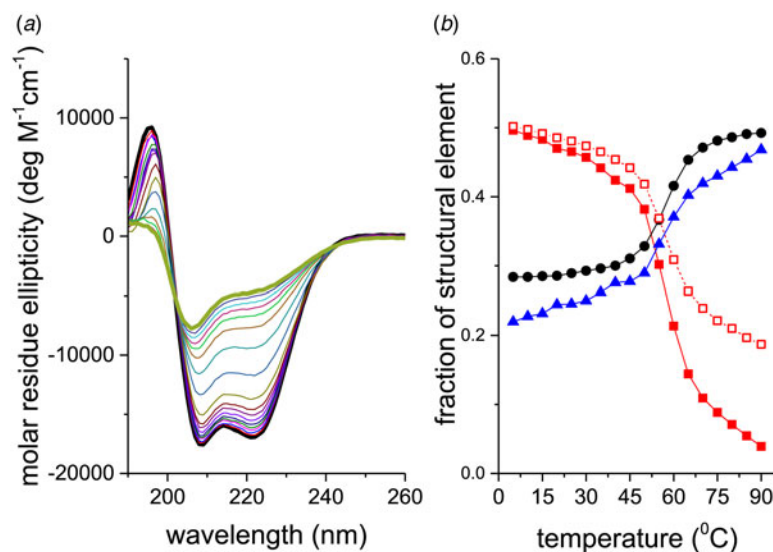


Fig. 2. Thermal unfolding of recombinant human Apo A-1 as seen by CD spectroscopy. The Apo A-1 concentration was 101 μM in PBS buffer adjusted to pH 7.4. The path length of the CD optical cell was 0.1 mm. (a) Far-UV CD spectra (buffer-subtracted) between 5 $^{\circ}\text{C}$ (black line) and 90 $^{\circ}\text{C}$ (olive line) recorded in 5 $^{\circ}\text{C}$ steps. (b) Analysis of the CD spectra. Spectral deconvolution: (■) α -helix, (●) β -sheet + β -turn, and (▲) random coil. (□) α -Helix content calculated with the ellipticity at 222 nm according to Eq. (24).

Different methods can be used to derive quantitative information on the progress of the protein unfolding reaction. The simplest protocol is to evaluate the mean residue ellipticity at $\lambda = 222$ nm since the unfolded protein is assumed to have no absorbance at this wavelength. The α -helix fraction, f_{α} is determined according to (Morriset *et al.* 1973)

$$f_{\alpha} = \frac{-\epsilon_{222\text{nm}} + 3000}{39\,000} \quad (24)$$

The corresponding analysis of the spectra of Fig. 2a is displayed in Fig. 2b (□). Equation (24) tends to overestimate the α -helix content, in particular if the α -helix content is low.

A more precise method is to deconvolute the CD spectra in terms of their α -helix-, β -sheet, β -turn, and random coil content. A CD fitting procedure based on 44 reference spectra (Reed & Reed, 1997) was applied to the spectra of Fig. 2a and the results are also shown in Fig. 2b. The α -helix content decreases from 50% to 4%, the random coil structure increases from 28% to 49%, and the β -structure (β -sheet + β -turn) increases from 22% to 47% (in the interval 5–90 $^{\circ}\text{C}$). The isodichroic point seen in Fig. 2 is not exactly confirmed in this structural analysis, which can be traced back to the 25% increase in β -structure with temperature.

If Apo A-1 unfolding is interpreted as a two-state process, it should be possible to quantitate the equilibrium by a linear combination of two limiting spectra. We assume that these are the 5 and 90 $^{\circ}\text{C}$ spectra, representing the folded and the unfolded Apo A-1, respectively. We define the fraction of native Apo A-1 as $\Theta_N = 1.0$ at 5 $^{\circ}\text{C}$ and $\Theta_N = 0$ at 90 $^{\circ}\text{C}$. Spectra at intermediate temperatures are then simulated by the weighted superposition of the two limiting spectra. An excellent fit of all spectra is indeed possible by this analysis. Figure 3a shows the variation of Θ_N with temperature (red dots).

Alternatively, the α -helix fraction, f_{α} (Fig. 2b), can also be interpreted in terms of a two-state equilibrium. We define the maximum α -helix content at 5 $^{\circ}\text{C}$ as f_N and the minimum α -helix content at 90 $^{\circ}\text{C}$ as f_U . The fraction of native protein is then given by $\Theta_N = (f_{\alpha} - f_U)/(f_N - f_U)$ and is also shown in Fig. 3a (black squares). A perfect agreement of the two methods is obtained even though f_{α} (α -helix fraction) considers only a single structural element, whereas the linear combination of spectra includes all structural elements.

The observation of an isodichroic point is usually taken as evidence for equilibrium between just two protein conformations, the native and the denatured, unfolded protein. However, an isodichroic point can also be generated by an *intramolecular* two-state equilibrium. Each peptide unit within a protein can exist in a native ‘folded’ and a denatured ‘unfolded’ conformation. The two conformations have different CD spectra. An increase in temperature shifts the intramolecular equilibrium of peptide units from folded to unfolded. This *intramolecular* equilibrium generates an isodichroic point. The protein solution

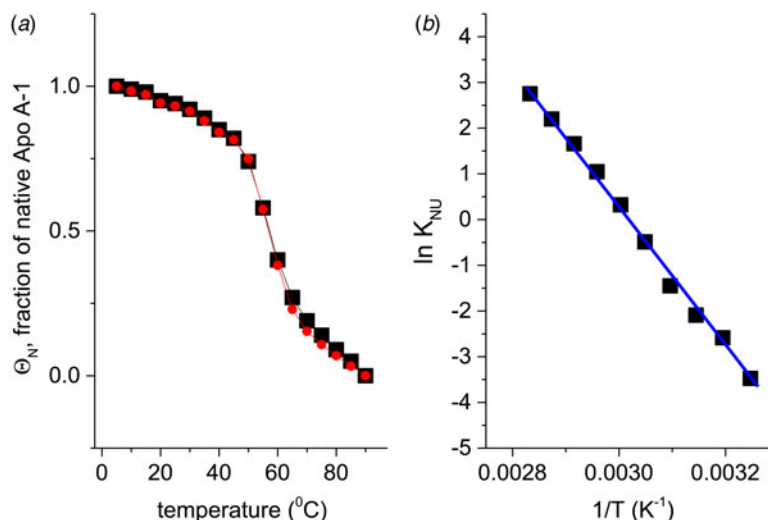


Fig. 3. (a) Two methods to quantitate the CD spectra of Fig. 2. (●) The spectra at 5 and 90 °C were linearly combined at different ratios to simulate the spectra at intermediate temperatures. Θ_N denotes the fraction of the 5 °C spectrum (= native Apo A-1) in the simulated spectrum. (■) The fraction of α -helix content, f_α , as evaluated with a CD fit program and normalized such that the spectrum at 5 °C corresponds to $\Theta_N = 1$ and that at 90 °C to $\Theta_N = 0$. (b) Data of panel a (limited to 35–80 °C) analysed with the two-state model. Equilibrium constant $K_{\text{NU}}(T) = (1 - \Theta_N)/\Theta_N$ (logarithmic scale) plotted as a function of $1/T$. $\Delta H_{\text{NU}}^0 = \Delta H_{\text{van't Hoff}} = 30.5 \text{ kcal mol}^{-1}$.

may contain protein molecules with many different conformations, ranging from all-helical to all-unfolded but the constituting peptide units fluctuate between just two conformations.

3.2 Two-state model applied to Apo A-1 unfolding

The binding constant $K_{\text{NU}}(T) = (1 - \Theta_N)/\Theta_N$ (Eq. (12)) can be calculated from the data of Fig. 3a for a limited temperature range of 35–80 °C. The equilibrium constant increases with temperature from $K_{\text{NU}} = 0.03$ at 35 °C to 16 at 80 °C. Figure 3b shows the corresponding van't Hoff plot of $\ln K$ versus $1/T$. The slope of the linear regression analysis yields an unfolding enthalpy of $\Delta H_{\text{NU}}^0 = 30.5 \text{ kcal mol}^{-1}$, in agreement with earlier studies (Gursky & Atkinson, 1996; Saito *et al.* 2003a; Tanaka *et al.* 2008).

The foregoing analysis is limited to the central region of the transition curve. The whole temperature range can be simulated with Eqs. (11) and (15) as shown in Fig. 4. The solid black line is the two-state model calculated with $\Delta H_{\text{NU}}^0 = 30 \text{ kcal mol}^{-1}$. The predicted transition curve fits the experimental data quite well in the transition region but deviates considerably in the region of high α -helix content.

As an aside it may be noted that a $\Delta C_{\text{p,NU}}^0 > 0$ term in Eq. (10) has no influence on the shape of the CD unfolding transition curve. This is explained by the fact that the contribution of the conformational enthalpy ΔH_{NU}^0 is much larger than that of $\Delta C_{\text{p,NU}}^0$. A $\Delta C_{\text{p,NU}}^0 > 0$ leads to a second unfolding transition at low temperatures ('cold denaturation') (Nicholson & Scholtz, 1996).

3.3 Zimm–Bragg theory applied to Apo A-1 unfolding

The recombinant human Apo A-1 has a chain length of 245 amino acids. Its α -helix content varies between $f_\alpha \sim 53 \pm 5\%$ at 10 °C and $\sim 5 \pm 2\%$ at 90 °C. The number of peptide units involved in the α -helix-to-random coil transition is $N \sim 115 \pm 10$.

Figure 4 shows the simulation of the CD unfolding curve with the Zimm–Bragg theory. The enthalpy for the formation of a helical peptide unit was set at $h = -1.1 \text{ kcal mol}^{-1}$. The other parameters were $\sigma = 6 \times 10^{-4}$, $T_\infty = 335 \text{ K}$, and $N = 120$. The Zimm–Bragg theory leads to a better fit to the spectroscopic data over the whole temperature range than the two-state model.

The Zimm–Bragg theory provides thermodynamic insight via the h -parameter. As $N \sim 120$ α -helical residues are unfolded, the expected enthalpy change is $\Delta H_{\text{NU}}^0 = N \times (-h) \sim 120 \times 1.1 \text{ kcal mol}^{-1} = 132 \text{ kcal mole}^{-1}$. This is much larger than the 30 kcal mol^{-1} deduced with the two-state model but very close to the calorimetric enthalpy of $\Delta H_{\text{exp}}^0 = 138 \text{ kcal mol}^{-1}$ obtained with DSC (see Section 4.1).

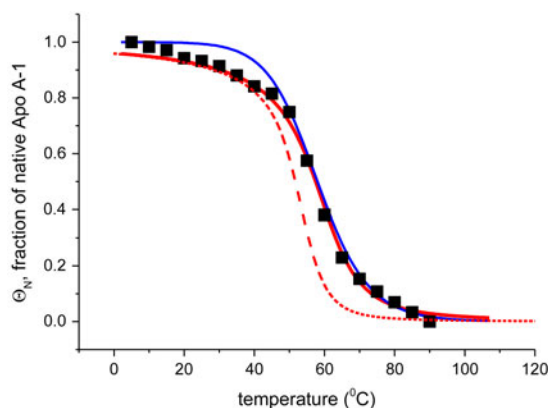


Fig. 4. Temperature-induced unfolding of recombinant Apo A-1 in PBS buffer. Comparison of the two-state model with the Zimm–Bragg theory. (■) Fraction of native Apo A-1 calculated from the change in α -helix content between 5 °C ($\Theta_{\text{helix}} = 1$) and 90 °C ($\Theta_{\text{helix}} = 0$) (experimental data of Fig. 3a). Solid blue line: prediction of the two-state model, with $\Delta H_{\text{NU}}^0 = 30.0 \text{ kcal mol}^{-1}$ and $T_0 = 331 \text{ K}$. Solid red line: Zimm–Bragg theory with nucleation parameter $\sigma = 6 \times 10^{-4}$, hydrogen bond enthalpy $h = -1.1 \text{ kcal mol}^{-1}$, $T_\infty = 335 \text{ K}$, $N = 120$. Dashed red line: Zimm–Bragg theory with the parameters yielding the best fit to the DSC data (see Fig. 7): $\sigma = 1.5 \times 10^{-4}$, $T_\infty = 331.1 \text{ K}$, $N = 120$.

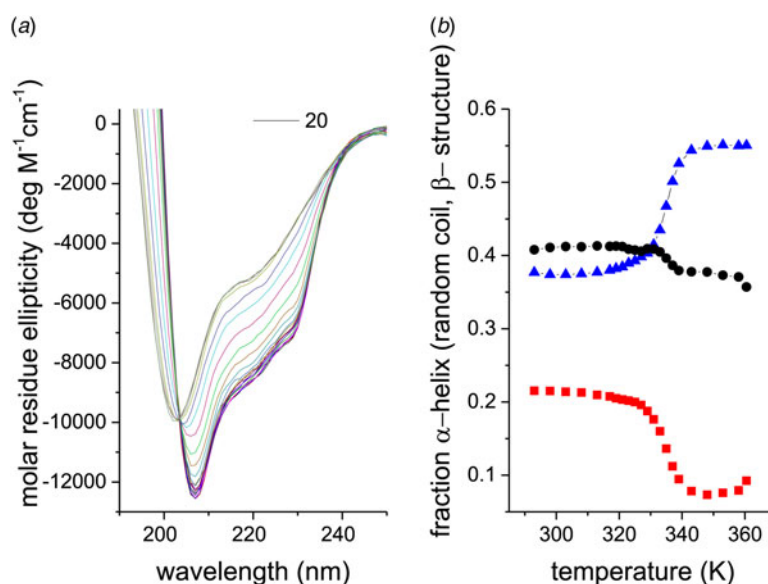


Fig. 5. (a) CD spectra of 10 μM egg-white lysozyme (20% glycine-HCl buffer, pH 2.5) recorded from 20 to 85 °C in 5 °C steps. (b) Analysis of the CD spectra in terms of three structural elements: (■) α -helix, (●) β -sheet + β -turn, and (▲) random coil.

3.4 Lysozyme unfolding. A globular protein with α/β -structure

Lysozyme is a globular protein with 129 amino acid residues and is the classical example of a two-state unfolding equilibrium (Kiefhaber, 1995; Miranker *et al.* 1991; Privalov, 1997; Radford *et al.* 1992).

The CD spectra of a 10 μM lysozyme solution are shown as a function of temperature in Fig. 5a. An isodichroic point is observed at 203 nm. The structural analysis is given in Fig. 5b. The α -helix content of the native protein is only 22% at 20 °C and decreases to 8% at 87 °C. As lysozyme is composed of 129 amino acids, at most ~ 20 – 30 peptide units are involved in the α -helix-to-random coil transition. The extent of β -structure is about 40% and decreases only little above the unfolding temperature.

The quantitative analysis of the CD spectra is based on the α -helix content (●) and the linear combination of the 20 and 85 °C spectra (■) (Fig. 6). The fraction of native protein, Θ_{N} , is plotted as a function of temperature. The midpoint of the unfolding

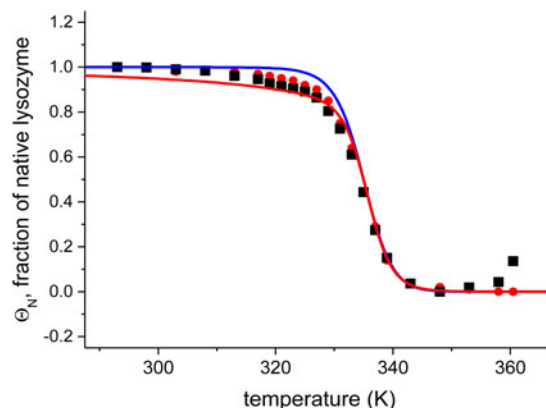


Fig. 6. Analysis of the CD spectra of lysozyme. (■) Linear combination of the 20 °C and the 85 °C spectra. The fraction of native lysozyme varies from $\Theta_N = 1$ at 20 °C to $\Theta_N = 0$ at 80 °C. (●) Θ_N calculated from the change in α -helix content. Solid blue line: two-state model using $\Delta H_{\text{NU}}^0 = 90.8 \text{ kcal mol}^{-1}$ and $T_0 = 335 \text{ K}$. Solid red line: Zimm–Bragg theory using the parameters derived from DSC measurements. $\sigma = 1.1 \times 10^{-6}$, $h = -1.1 \text{ kcal mol}^{-1}$, $\Delta C_{\text{p,NU}}^0 = 2.27 \text{ kcal mol}^{-1}$, and $N = 129$ (see Fig. 8).

transition is at $T_0 = 335 \text{ K} = 62 \text{ °C}$, in agreement with earlier reports (Privalov *et al.* 1995). The unfolding of lysozyme occurs between 40 and 70 °C and the transition is clearly sharper than that of Apo A-1.

Application of the two-state model (Fig. 6, solid blue line) yields an unfolding enthalpy of $\Delta H_{\text{NU}}^0 = 90.5 \text{ kcal mol}^{-1}$.

In order to apply the Zimm–Bragg theory, we consider the unfolding of lysozyme as a change from ‘folded’ peptide units to ‘unfolded’ peptide units involving all 129 peptide units. The caloric heat of unfolding as measured with DSC and discussed below is $\Delta H_{\text{exp}}^0 = 138 \text{ kcal mol}^{-1}$, yielding an enthalpy change of $138/129 = 1.07 \text{ kcal mol}^{-1}$ per peptide unit. This is close to the enthalpy for the opening of a hydrogen bond. However, as discussed above, energy calculations show that the major energy of α -helix and β -structure formation comes from van-der-Waals interactions and the hydrophobic effect (Yang & Honig, 1995a, b). We therefore postulate an enthalpy difference between ‘unfolded’ and ‘folded’ peptide units of $h = -1.1 \text{ kcal mol}^{-1}$, independent of the specific nature of the protein. The total enthalpy of unfolding is determined by the number of involved peptide units. The quantitative analysis of lysozyme is then based on the full length protein (red line in Fig. 6) with $\sigma = 1.1 \times 10^{-6}$ and $h = -1.1 \text{ kcal mol}^{-1}$. These simulation parameters are identical to those derived from DSC measurements (discussed in detail in Fig. 8). The Zimm–Bragg theory provides an excellent fit of the CD unfolding curve of lysozyme.

3.5 Sloping baselines in CD spectroscopy

Inspection of Figs 1–5 reveals sloping CD baselines at the beginning and the end of the unfolding transition. This effect is quite pronounced for Apo A-1 with its rather broad transition but occurs also to a lesser extent for the highly cooperative lysozyme. Special algorithms have been proposed to fit ‘sloping baselines’ (Gursky, 2015; Santoro & Bolen, 1988). However, sloping baselines could also be the result of the cooperativity of the system. It may be noted that sloping baselines are better accounted for by the Zimm–Bragg theory than by the two-state model (see Supplementary Information S1, S5, S6, S9, S12). The definition of the beginning and end of the conformational transition has a distinct influence on the van’t Hoff enthalpy determined with the two-state model. The narrower the selected temperature range, the steeper is the slope of the transition curve and the larger the van’t Hoff enthalpy.

4. Thermal unfolding measured with DSC

4.1 Calorimetry of Apo A-1

The thermal unfolding of lipid-free recombinant Apo A-1 was measured between 10 and 90 °C. Figure 7 (black line) shows the DSC scan of a 100 μM Apo A-1 solution after subtracting the buffer baseline. The molar heat capacity reaches a maximum at the midpoint of the unfolding transition ($T_0 = 52.5 \text{ °C}$). The unfolded protein has a larger heat capacity than the native protein with $\Delta C_{\text{p,NU}}^0 = 2.508 \text{ kcal mol}^{-1}$. The unfolding process is completely reversible in the temperature interval of 10–90 °C. Three consecutive DSC scans gave identical results (Schulthess *et al.* 2015; Zehender *et al.* 2012).

The conformational change occurs between 30 and 70 °C. The area under the $C_{\text{p}}(T)$ versus T curve in this interval yields an unfolding enthalpy of $\Delta H_{\text{exp}}^0 = 138.4 \text{ kcal mole}^{-1}$. It includes the conformational change proper and the contribution of the

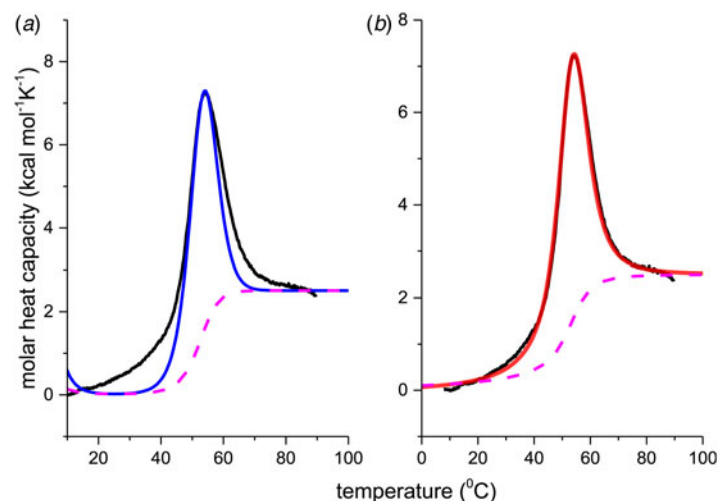


Fig. 7. Differential scanning calorimetry (DSC) of recombinant ApoA-1 (100 μM) in PBS buffer pH 7.4. Molar heat capacity, $C_p(T)$, as a function of temperature. The C_p maximum occurs at 52.4 $^{\circ}\text{C}$ and the increase in heat capacity between native and unfolded Apo A-1 is $\Delta C_{p,\text{NU}}^0 = 2.508 \text{ kcal mol}^{-1} \text{ K}^{-1}$. The heating rate was 1 $^{\circ}\text{C min}^{-1}$ and 3 consecutive scans were virtually identical. Solid black line: experimental DSC scan (identical in panels *a* and *b*). The total heat of unfolding between 30 $^{\circ}\text{C}$ and 70 $^{\circ}\text{C}$ is $\Delta H_{\text{exp}}^0 = 138.9 \text{ kcal mol}^{-1}$. (*a*) Two-state model (blue line). $T_0 = 52.4 \text{ }^{\circ}\text{C}$, $\Delta H_{\text{NU}}^0 = 68.1 \text{ kcal mol}^{-1}$. The total heat of unfolding is $\Delta H_{2\text{-state}}^0 = \Delta H_{\text{NU}}^0 + \Delta H_{\text{Cp,NU}}^0 = 113.4 \text{ kcal mol}^{-1}$. (*b*) Zimm–Bragg theory (red line). $\sigma = 1.5 \times 10^{-4}$, $h = -1.1 \text{ kcal mol}^{-1}$, $N = 120$, $\Delta C_{p,\text{NU}}^0 = 2.508 \text{ kcal mol}^{-1}$, $T_{\infty} = 331.1 \text{ K}$. The total heat of unfolding is $\Delta H_{\text{cal}}^0 = 135.4 \text{ kcal mol}^{-1}$. Dashed magenta lines: contributions of $\Delta C_{p,\text{NU}}^0$ to the total heat capacity, calculated with either two-state model (*a*) or the Zimm–Bragg theory (*b*).

increased heat capacity. As seen by CD spectroscopy ~ 120 amino acids participate in the transition and the contribution of each peptide unit is $1.13 \text{ kcal mol}^{-1}$.

The change in the molar heat capacity, $\Delta C_{p,\text{NU}}^0$, is usually not detected in spectroscopic measurements. It is however essential for the analysis of the thermodynamic equilibrium. The *total* heat of unfolding, not only the conformational enthalpy, must be considered for the molecular interpretation of the folding \rightleftharpoons unfolding equilibrium. ‘It is clear that in considering the energetic characteristics of protein unfolding one has to take into account all energy which is accumulated upon heating and not only the very substantial heat effect associated with gross conformational transitions, that is, all the excess heat effects must be integrated’ (Privalov & Dragan, 2007).

We analyzed the DSC unfolding experiment with the two models introduced above, taking into account the contribution of $\Delta C_{p,\text{NU}}^0$ in both cases. The simulation with the two-state model is presented in Fig. 7*a*. The fit parameters are $T_0 = 52.4 \text{ }^{\circ}\text{C}$, $\Delta H_{\text{NU}}^0 = 66.9 \text{ kcal mol}^{-1}$ and $\Delta C_{p,\text{NU}}^0 = 2.508 \text{ kcal mol}^{-1} \text{ K}^{-1}$ and are in agreement with previous DSC measurements (Schulthess *et al.* 2015; Tall *et al.* 1975, 1976). The contribution of the $\Delta C_{p,\text{NU}}^0$ term to the unfolding process is given by the area under the dashed magenta line in Fig. 7*a* and is $\Delta H_{\text{Cp,NU}}^0 = 45.2 \text{ kcal mol}^{-1}$. This yields a total unfolding enthalpy of $112.0 \text{ kcal mol}^{-1}$, which is 20% smaller than the experimental result $\Delta H_{\text{exp}}^0 = 138.4 \text{ kcal mol}^{-1}$.

The conformational enthalpy of $\Delta H_{\text{NU,DSC}}^0 = 66.9 \text{ kcal mol}^{-1}$ deduced with the two-state model is more than twice as large as that deduced with the same model from CD spectroscopic ($\Delta H_{\text{NU,CD}}^0 = 30 \text{ kcal mol}^{-1}$). A much sharper transition is recorded in DSC than in CD spectroscopy.

The simulation of the DSC experiment with the Zimm–Bragg theory (Fig. 7*b*) provides a perfect fit of the unfolding transition. The midpoint of the transition, $\Theta_{\text{helix}} = 1/2$, is predicted at $T_0 = 52.4 \text{ }^{\circ}\text{C}$, in agreement with the DSC maximum. Integration of the Zimm–Bragg curve in the interval 30–70 $^{\circ}\text{C}$ yields a total transition enthalpy of $\Delta H_{\text{calc,ZB}}^0 = 135.4 \text{ kcal mol}^{-1}$, in excellent agreement with the experimental result. The contribution of $\Delta C_{p,\text{NU}}^0$ to the unfolding enthalpy is $\Delta H_{\text{Cp,NU}}^0 = 50.0 \text{ kcal mol}^{-1}$ and the conformational enthalpy is $\Delta H_{\text{NU,ZB}}^0 = 85.4 \text{ kcal mol}^{-1}$.

4.2 Calorimetry of lysozyme

Figure 8 shows the DSC result of a 50 μM lysozyme solution at pH 2.5. The molar heat capacity change of $\Delta C_{p,\text{NU}}^0 = 2.27 \text{ kcal mol}^{-1} \text{ K}^{-1}$ is in agreement with previous measurements reporting 1.54–2.2 $\text{kcal mol}^{-1} \text{ K}^{-1}$ (Myers *et al.* 1995; Privalov & Gill, 1988; Privalov & Makhatadze, 1990; Privalov *et al.* 1995; Rosgen & Hinz, 2000). The midpoint of the unfolding process is at

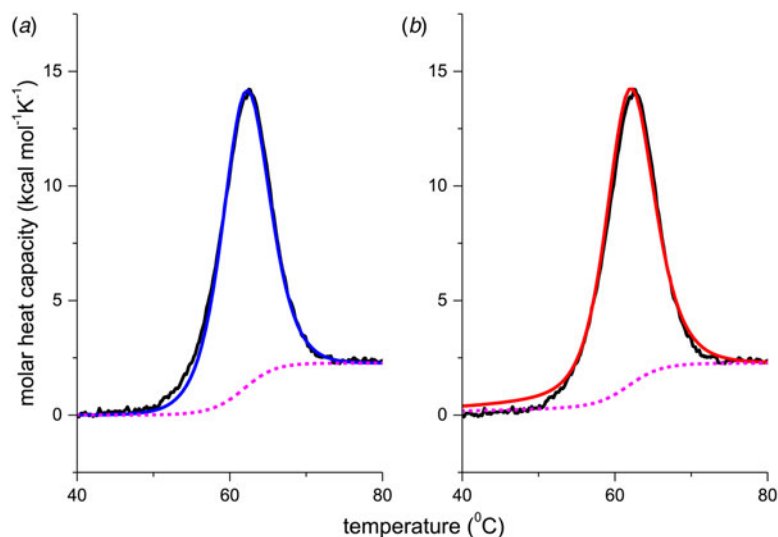


Fig. 8. Differential scanning calorimetry of lysozyme. Analysis of thermal unfolding with (a) the two-state model and (b) the Zimm–Bragg theory. The experimental result (black line) is the DSC scan of a 50 μM lysozyme solution in 20% glycine buffer, pH 2.5, measured at a heating rate of 1 $^{\circ}\text{C min}^{-1}$. (a) Two-state model (blue line). $T_0 = 335 \text{ K} = 62 \text{ }^{\circ}\text{C}$, $\Delta H_{\text{NU}}^0 = 106.9 \text{ kcal mol}^{-1}$, $\Delta C_{\text{p,NU}}^0 = 2.269 \text{ kcal mol}^{-1}\text{K}^{-1}$. (b) Zimm–Bragg theory (red line). $\sigma = 1.1 \times 10^{-6}$, $h = -1.10 \text{ kcal mol}^{-1}$, $N = 129$, $\Delta C_{\text{p,NU}}^0 = 2.269 \text{ kcal mol}^{-1}$, $T_{\infty} = 349.5 \text{ K} = 76.5 \text{ }^{\circ}\text{C}$. The dashed magenta line shows the contribution of $\Delta C_{\text{p,NU}}^0$ to the transition calculated with the two-state model (a) or the Zimm–Bragg theory (b).

$T_0 = 61.8 \text{ }^{\circ}\text{C}$, which is identical with the CD measurement. Integration of the experimental $C_p(T)$ versus T transition curve between 50 and 73 $^{\circ}\text{C}$ yields an unfolding enthalpy of $\Delta H_{\text{exp}}^0 = 136.4 \text{ kcal mol}^{-1}$.

Figure 8a shows the simulation with the two-state model (solid blue line) using $\Delta H_{\text{NU,DSC}}^0 = 106.9 \text{ kcal mol}^{-1}$. The dashed magenta line shows the contribution of $\Delta C_{\text{p,NU}}^0$ to the unfolding transition, which is $\Delta H_{\text{Cp,NU}}^0 = 26.9 \text{ kcal mol}^{-1}$. The sum $\Delta H_{\text{cal,2-state}}^0 = \Delta H_{\text{NU,DSC}}^0 + \Delta H_{\text{Cp,NU}}^0 = 133.8 \text{ kcal mol}^{-1}$ is consistent with the experimental result for the total heat change. The two-state model provides a good fit of lysozyme unfolding (Privalov *et al.* 1995). However, the conformational enthalpy deduced with DSC, $\Delta H_{\text{NU,DSC}}^0 = 106.9 \text{ kcal mol}^{-1}$, is again larger than that determined with CD spectroscopy, $\Delta H_{\text{NU,CD}}^0 = 90.5 \text{ kcal mol}^{-1}$.

The simulation with the Zimm–Bragg theory is displayed in Fig. 8b. We assume that all $N = 129$ amino acid residues participate in the cooperative ‘folded’ \rightleftharpoons ‘unfolded’ equilibrium with an unfolding enthalpy of $h = 1.1 \text{ kcal mol}^{-1}$. As the experimental heat of unfolding is $\Delta H_{\text{exp}}^0 = 138.2 \text{ kcal mol}^{-1}$ $h = 1.1 \text{ kcal mol}^{-1}$ is consistent with the experimental result of $138.2/129 = 1.07 \text{ kcal mol}^{-1}$. A perfect simulation of the experimental data is achieved with $\sigma = 1.1 \times 10^{-6}$, $N = 129$, $\Delta C_{\text{p,NU}}^0 = 2.27 \text{ kcal mol}^{-1}$ and $T_{\infty} = 349.5 \text{ K} = 76.5 \text{ }^{\circ}\text{C}$, predicting a total enthalpy of $\Delta H_{\text{cal,ZB}}^0 = 139.9 \text{ kcal mol}^{-1}$.

Figure 8 demonstrates that the DSC data can be explained almost equally well by the two-state model and the Zimm–Bragg theory. However, the Zimm–Bragg theory fits the CD spectroscopy unfolding curve (Fig. 6) with exactly the same parameters as used for the DSC measurements. In contrast, the two-state model requires different conformational unfolding enthalpies ΔH_{NU}^0 for DSC ($106.9 \text{ kcal mol}^{-1}$) and CD ($90.7 \text{ kcal mol}^{-1}$).

4.3 A 50-amino acid peptide

Remarkable differences between the two-state model and the Zimm–Bragg theory are found for a short synthetic 50-amino acid peptide with sequence Ac-Y(AEAAKA)₈F-NH₂. The peptide is almost completely α -helical at 0 $^{\circ}\text{C}$ and shows a very broad unfolding transition centered at 42 $^{\circ}\text{C}$ (Scholtz, 1991; Scholtz *et al.* 1991a, b). Figure 9a displays the temperature-dependence of the ellipticity at 222 nm (Scholtz *et al.* 1991a). The α -helix fraction, calculated according to Eq. (24), is $f_{\alpha} = 0.98$ at 0 $^{\circ}\text{C}$ and 0.23 at 80 $^{\circ}\text{C}$. No plateau is reached at 80 $^{\circ}\text{C}$ and the shape of the transition curve suggests $f_{\alpha} = 0$ at high temperatures. We therefore assume that all 50 amino acid residues participate in the α -helix-to-random coil transition. The ellipticity is linearly proportional to the helix fraction according to $\epsilon_{222\text{nm}} (\text{degM}^{-1} \text{ cm}^{-1}) = -39000 \Theta_{\text{helix}}$. The helix fraction can then be calculated with either the two-state model (blue line in Fig. 9a) or the Zimm–Bragg theory (red line in Fig. 9a). An almost perfect fit of the CD transition curve is obtained with both models. The two-state model requires an

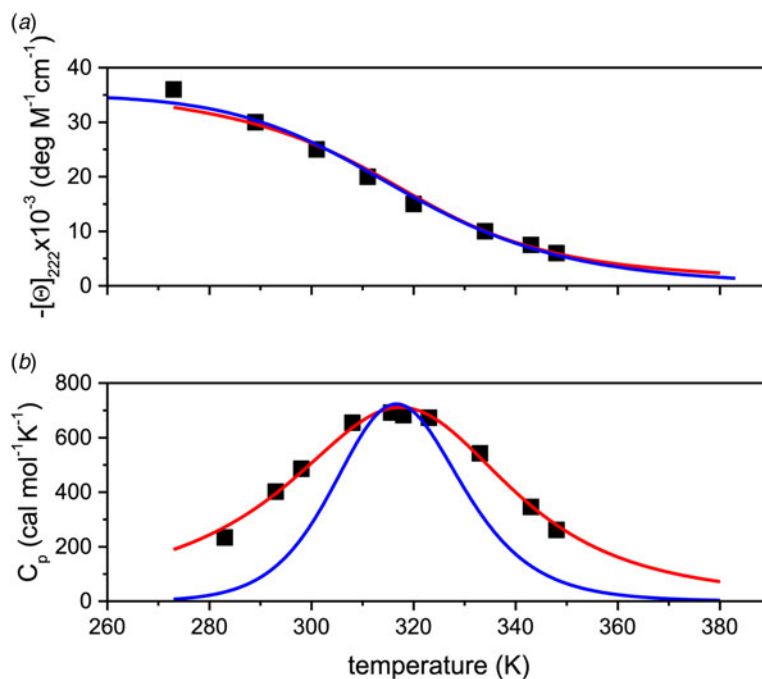


Fig. 9. Thermal unfolding of the 50-residue peptide Ac-Y (AEAAKA)₈F-NH₂. (a) Circular dichroism spectroscopy at 222 nm. (b) Molar heat capacity, $C_p(T)$, as determined with differential scanning calorimetry. (■) Experimental data. The red solid lines in both panels were calculated with the Zimm–Bragg theory using the same set of parameters: $N = 50$, $\sigma = 4 \times 10^{-3}$, $h = -0.93$ kcal mol⁻¹, $T_\infty = 326$ K. Solid blue lines are the predictions of the two-state model calculated with (a) $\Delta H_{\text{NU}}^0 = 12$ kcal mol⁻¹, (b) $\Delta H_{\text{NU}}^0 = 24$ kcal mol⁻¹ and $T_0 = 317.5$ K.

unfolding enthalpy of $\Delta H_{\text{NU}}^0 = 12$ kcal mol⁻¹. The Zimm–Bragg theory uses $N = 50$, $\sigma = 4 \times 10^{-3}$, $h = -0.93$ kcal mol⁻¹, and $T_\infty = 325$ K ($\Delta C_{p,\text{NU}}^0 = 0$).

Figure 9b displays the calorimetric data (Fig. 4 in (Scholtz, 1991; Scholtz *et al.* 1991a)). The large width of the transition requires assumptions about the baseline and restricts the accuracy of the calorimetric analysis. The calorimetric heat deduced from the experimental data is $\Delta H_{\text{cal}} = 45.8$ kcal mol⁻¹ (Table 2 in (Scholtz *et al.* 1991a)).

The solid red line in Fig. 9b is the interpretation of the experimental data with the Zimm–Bragg theory. Exactly the same parameters are used for the DSC transition as listed above for the CD transition curve. The calculated enthalpy of unfolding is $\Delta H_{\text{NU}}^0 = 46.1$ kcal mol⁻¹, in excellent agreement with the calorimetric result.

The solid blue line in Fig. 9b shows the fit with the two-state model with $\Delta H_{\text{NU}}^0 = 27$ kcal mol⁻¹. The maximum C_p value is reached, but the fit of the whole transition curve is poor. It is obvious that the two-state model fails to reproduce the DSC data.

Scholtz *et al.* compared the CD spectra of the 50-amino acid peptide with those of shorter fragments (Scholtz *et al.* 1991b). They used $\sigma = 3.3 \times 10^{-3}$, $h = -0.955$ kcal mol⁻¹ and $T_\infty = 329$ K, consistent with the present analysis.

4.4 Proteins selected from the literature

The comparison between the two-state model and the Zimm–Bragg theory was extended to protein unfolding experiments reported in the literature. Most useful were studies where both CD and DSC data were available and where the increased heat capacity of the unfolded protein was also measured. Examples are pseudo wild-type T4 lysozyme and its mutant S44[A] T4-lysozyme (Carra *et al.* 1996), the aspartate receptor C-fragment and its mutant S461L (Seeley *et al.* 1996; Wu *et al.* 1995) and β -lactoglobulin (Garcia-Hernandez *et al.* 1998).

High quality DSC data of lysozyme (Privalov *et al.* 1995; Rosgen & Hinz, 2000), RNase (Rosgen & Hinz, 2000), ubiquitin (Privalov & Dragan, 2007), myoglobin (Privalov & Makhatadze, 1993) and β -lactoglobulin (Schwarz, 1990) were also analysed, even though no CD spectra were available.

In all publications the authors used the two-state model for the interpretation of the experimental results. As the data were only available as printed figures, the corresponding traces were enlarged and digitized manually (see Supplementary Information Figs S1–S17) Table 1 summarises the experimental parameters deduced from these figures. Some protein

Table 1. Differential scanning calorimetry and CD spectroscopy of protein unfolding. Experimental results^a

	$N_{\text{amino acids}}$	$T_{\text{ini}} - T_{\text{end}}$ (K)	ΔT (K)	$T_{0,\text{DSC}}$ (K)	$T_{0,\text{CD}}$ (K)	$\Delta C_{\text{p,NU}}^0$ (kcal/molK)	ΔH_{exp}^0 (kcal mol ⁻¹) ^b	Comment	Reference
50-amino acid peptide	50	243–383	140	317.5	317.5	0	33.2 (truncated, 10–75 °C)	DSC: Fig. 8a CD: Fig. 8b	Scholtz (1991), Scholtz <i>et al.</i> (1991a)
Aspartate receptor fragment	297	293–348	55	324	318	0.82	107.2	Sup. Info. 1	Seeley <i>et al.</i> (1996), Wu <i>et al.</i> (1995)
Ubiquitin pH 2.0	76	310–351	41	329		0.814	70.8	Sup. Info. 2	Privalov & Dragan (2007)
Ubiquitin pH 3.0	76	326–368	42	347		0.48	76.3	Sup. Info. 3	Ibarra-Molero <i>et al.</i> (1999a)
Ubiquitin pH 3.0	76	323–365	42	347		0.573	78.9	Sup. Info. 4	Privalov & Dragan (2007)
Apo A1	245	303–343	40	325.5	331.2	2.508	138.9	CD: Fig. 4 DSC: Fig. 6	This work
S461L aspartate receptor fragment	297	313–353	40	333	330	0	64.1	Sup. Info. 5	Seeley <i>et al.</i> (1996), Wu <i>et al.</i> (1995)
β -lactoglobulin pH 1.1	162	333–373	40	352.5	344.5	0	92.5	Sup. Info. 6	Garcia-Hernandez <i>et al.</i> (1998)
β -lactoglobulin pH 2.5	162	343–378	35	360.7		0	96	Sup. Info. 7	Garcia-Hernandez <i>et al.</i> (1998)
β -lactoglobulin pH 3.3	162	333–373	40	360.7		4.538	156.5	Sup. Info. 8	Schwarz (1990)
S44[A]T4 lysozyme	165	308–343	35	327.6	321.6	1.218	131.8	Sup. Info. 9	Carra <i>et al.</i> (1996)
RNase	124	303–333	30	317.3		0.884	101.5	Sup. Info. 10	Rosgen & Hinz (2000)
Lysozyme pH 1.9	129	313–341.5	28.5	328.3		1.839	132.7	Sup. Info. 11	Rosgen & Hinz (2000)
Ubiquitin (bovine) pH 4.0	76	350–378	28	363		0.74	83.8	Sup. Info. 12	Ibarra-Molero <i>et al.</i> (1999b)
Ubiquitin pH 4.0	76	345–378	33	363.2		0.597	90.2	Sup. Info. 13	Privalov & Dragan (2007)
Lysozyme pH 2.5	129	323–347.5	24.5	336.8		1.672	149.5	Sup. Info. 14	Fig. 8 ; Privalov <i>et al.</i> (1995)
Lysozyme pH 2.5	129	323–347	24	336.5		2.317	136.0	Sup. Inf. 15	Fig. 7 ; Privalov <i>et al.</i> (1995)
Lysozyme pH 2.5	129	323–346	23	335	335	2.269	143.5	CD; Fig. 5 DSC: Fig. 8	This work
Myoglobin	153	333–356	23	349.5		2.866	153.8	Sup. Info. 16	Privalov <i>et al.</i> (1986)
Pseudo WT T4	164	318–335	17	327.5	322.5	2.508	158.1	Sup. Info. 17	Carra <i>et al.</i> (1996)

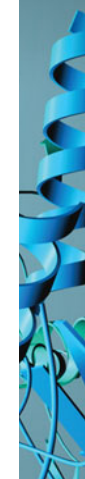
^a Proteins are ordered according to decreasing width of the unfolding transition.^b Experimental heat of protein unfolding includes the contribution of the heat capacity term.

Table 2. Two-state model. Comparison of DSC and CD spectroscopy data

	$T_{0,DSC}$ (K)	$T_{0,CD}$ (K)	ΔH_{exp}^0 (kcal mol ⁻¹)	$\Delta H_{NU,DSC}^0$ (kcal mol ⁻¹)	ΔH_{lit}^{DSC} (kcal mol ⁻¹)	$\Delta H_{NU,CD}^0$ (kcal mol ⁻¹)	$\Delta H_{Cp,NU}^0$ (kcal mol ⁻¹)	$\Delta H_{calc}^0 = \Delta H_{NU,DSC}^0 + \Delta H_{Cp,NU}^0$ (kcal mol ⁻¹)	ΔG_{NU}^0 (kcal mol ⁻¹)	rel error %	Comments
50-amino acid peptide	317.5	317.5	33.2 (truncated, 10–75 °C)	24.0		12.0	0.0	24.0			Scholtz (1991), Scholtz <i>et al.</i> (1991a) no fit of DSC possible, good fit CD, see Fig. 9
Aspartate receptor fragment	324	318	107.2	50.2	54 ± 7	35	19.9	70.1	8.04	34	Seeley <i>et al.</i> (1996), Wu <i>et al.</i> (1995) poor fit; Sup. Info S1
Ubiquitin pH 2.0	329		70.8	50.2	48		18.1	68.3	6.28	3.5	Privalov & Dragan (2007) Sup. Info S2
Ubiquitin pH 3.0	347		76.3	60.9	64		10.1	71.0	7.85	7	Ibarra-Molero <i>et al.</i> (1999a) Sup. Info. S3
Ubiquitin pH 3.0	347		78.9	63.3	64		10.4	73.7	10.3	6.6	Privalov & Dragan (2007) Sup. Info. S4
Apo A-1	325.5	331.2	138.9	68.1	64 ± 8.9	30.1	45.2	113.4	3.75	18.1	This work, see Fig. 7a, Tall <i>et al.</i> (1976)
S461L aspartate receptor fragment	333	331	64.1	61.6	61 ± 11	61.6	0	61.6	7.43	3.9	Seeley <i>et al.</i> (1996), Wu <i>et al.</i> (1995) Sup. Info. S5
β -lactoglobulin pH 1.1	352.5	344.5	92.5	76.4	77.0	43	0	76.4	8.65	16.4	Delbaere <i>et al.</i> (1993) Sup. Info S6
β -lactoglobulin pH 2.5	360.7		96	87.2	87.1		0	87.2	8.49	9.1	Delbaere <i>et al.</i> (1993) Sup. Info S7
β -lactoglobulin pH 3.3	360.7		156.5	94.3	93.5		54	148.3	6.5	5.0	Jia <i>et al.</i> (1993) Sup. Info. S8
S44[A]T4 lysozyme	327.6	320	131.8	83.6	85.0	64	18.9	102.5	8.71	22.2	Carra <i>et al.</i> (1996) Sup. Info. S9
RNase	317.3		101.5	76.4	76.3		13.9	90.3	7.23	11	Rosgen & Hinz (2000) Sup. Info. S10
Lysozyme pH 1.9	328.3		132.7	92.7	89.5		24.5	117.2	8.04	11.7	Rosgen & Hinz (2000) Sup. Info. S11
Ubiquitin pH 4.0	363		83.8	70.9	71.4		11.1	82	5.48	2.1	Ibarra-Molero <i>et al.</i> (1999b) Sup. Info. S12
Ubiquitin pH 4.0	363		90.2	73.3	72		8.9	82.2	6.62	8.9	Privalov & Dragan (2007) Sup. Info. S13
Lysozyme pH 2.5 Fig. 8	336.8		149.5	113.2	115.1		18.0	131.2	8.1	12.2	Fig. 8, Privalov <i>et al.</i> (1995) Sup. Info. S14
Lysozyme pH 2.5 Fig. 6	336.5		136	104.6	115.1		24.6	129.2	7.2	5	Fig. 7, Privalov <i>et al.</i> (1995) Sup. Info. S15
Lysozyme pH 2.5	335	335	143.5	106.9	(114.9)	90.8	25.2	132.1	7.25	7.9	This work, see Fig. 8
Myoglobin pH 10.7	349.5		153.8	125.3	134.7		19.1	144.5	7.48	6.0	Privalov & Makhatadze (1993) Sup. Info. S16
Pseudo WT T4 lysozyme	327.5	322	158.1	125.4	127.5	120.6	19.0	144.4	6.4	8.7	Carra <i>et al.</i> (1996) Sup. Info S17



(lysozyme, ubiquitin, and β -lactoglobulin) were measured by different groups. Table 1 illustrates the variability of the different measurements.

Table 1 lists the width of the transition, ΔT , the calorimetric and spectroscopic midpoint temperatures, $T_{0,DSC}$ and $T_{0,CD}$, and the total heat of unfolding, ΔH_{exp}^0 . ΔH_{exp}^0 was determined by numerical integration of the digitized DSC curve in the transition interval. Table 1 further includes the change in the molar heat capacity, $\Delta C_{p,NU}^0$. The proteins are ordered according to decreasing width of the unfolding transition, indicating increasing cooperativity.

The extracted DSC and CD spectroscopy unfolding transitions were analysed with the two models. The results are summarized in Table 2 for the two-state model and in Table 3 for the Zimm–Bragg theory.

In Table 2 the enthalpy $\Delta H_{NU,DSC}^0$ is compared with available literature data, ΔH_{lit}^{DSC} , also obtained with the two-state model. Table 2 also contains $\Delta H_{Cp,NU}^0$, the contribution of the $\Delta C_{p,NU}^0$ term to the unfolding transition. The total unfolding enthalpy is $\Delta H_{NU,DSC}^0 + \Delta H_{Cp,NU}^0$ and must be compared with ΔH_{exp}^0 . The unfolding transitions measured with CD spectroscopy were also analysed and the corresponding conformational enthalpies are listed as $\Delta H_{NU,CD}^0$.

Table 3 contains the parameters of the Zimm–Bragg theory such as the number of peptide units N_{ZB} , the enthalpy per peptide unit h , the nucleation parameters σ_{DSC} and σ_{CD} , and the characteristic temperature T_{∞} . The predicted total enthalpy of unfolding is $\Delta H_{calc,ZB}^0$ and the corresponding free energy $\Delta G_{NU,ZB}^0$.

5. Cooperative unfolding and two-state model applied to DSC and CD spectroscopy

DSC is the method of choice for the thermodynamic analysis of protein unfolding. The integration of the C_p versus T calorimetric transition curve yields the total enthalpy of the unfolding reaction, ΔH_{exp}^0 . It comprises the so-called conformational enthalpy, ΔH_{NU}^0 , and the enthalpy contribution $\Delta H_{Cp,NU}^0$, caused by the increase in heat capacity. The unfolding ‘process results in a significant increase in heat capacity, by a value that does not depend noticeably either on temperature or on environmental conditions and is specific for the given protein’ (Privalov & Makhatadze, 1993). No unfolding model is required to evaluate ΔH_{exp}^0 .

5.1 The total heat of unfolding ΔH_{exp}^0

A first criterion for the quality of the two-state model and the Zimm–Bragg theory is their capability to reproduce the shape and the total enthalpy of the DSC transition curve. In Fig. 10 the enthalpies calculated with the Zimm–Bragg theory and the two-state model are plotted against the experimental result, ΔH_{exp}^0 . Linear regression analysis of the Zimm–Bragg data yields a straight line through the origin with slope $m = 1$ (average deviation $2.1 \pm 1.7\%$). The two-state model shows a larger scatter and regression analysis that yields a slope of $m = 0.89$ only. The two-state model systematically underestimates the total heat of unfolding, ΔH_{exp}^0 , by about 11%. The results of the two-state model are particularly poor for broad transitions. For the 50-amino acid peptide a fit with a single two-state model was not possible (see Fig. 9).

5.2 Equivalence of DSC and CD spectroscopy unfolding transitions?

A second quality criterion follows from a comparison of DSC and CD spectroscopy unfolding transitions obtained for a given protein under identical experimental conditions. If DSC and CD spectroscopy indeed report the same physical process, the simulation of the two unfolding transitions should be possible with identical thermodynamic parameters. The critical parameter for this comparison is the cooperativity, measured by the nucleation parameter σ of the Zimm–Bragg theory and the conformational enthalpy ΔH_{NU}^0 of the two-state model.

Figure 11a shows a plot of the nucleation parameter σ_{CD} , deduced from CD measurements, versus σ_{DSC} , obtained from DSC. The 50-amino acid peptide and the aspartate receptor fragment have broad transitions with nucleation parameters of $\sigma = 4 \times 10^{-3}$ and $\sigma = 1 \times 10^{-3}$, respectively. At the other extreme, pseudo WT T4 lysozyme has the sharpest transition with $\sigma = 5 \times 10^{-7}$. For 6 of the 7 proteins identical nucleation parameters σ_{DSC} and σ_{CD} are obtained. Linear regression analysis yields a straight line through the origin with slope $m = 1$. It can be concluded that (i) DSC and CD spectroscopy report the same transition, and (ii) the Zimm–Bragg theory describes both transitions with the same set of thermodynamic parameters. The only exception in Fig. 11a is Apo A-1, which shows a distinctly broader transition in CD spectroscopy than in DSC.

The two-state model uses the conformational enthalpy, ΔH_{NU}^0 (van’t Hoff enthalpy) as fit parameter. The larger ΔH_{NU}^0 , the sharper is the predicted transition curve. In Fig. 11b the CD parameter, $\Delta H_{NU,CD}^0$, is plotted against the DSC parameter, $\Delta H_{NU,DSC}^0$. The scatter of the data is considerable and the average deviation is $24 \pm 18\%$. The straight line through the origin has a slope of $m = 0.81$, indicating that the enthalpy deduced with CD spectroscopy systematically underestimate the

Table 3. Differential scanning calorimetry of protein unfolding analysed with the Zimm–Bragg theory

	N_{ZB}	h (kcal mol ⁻¹)	σ	σ_{CD}	T_{∞} (K)	ΔH_{exp}^0 (kcal mol ⁻¹)	$\Delta H_{\text{calc.ZB}}^0$ (kcal mol ⁻¹)	$\Delta H_{\text{Cp,NU}}^0$ (kcal mol ⁻¹)	$\Delta G_{\text{NU,ZB}}^0$ ^a (kcal mol ⁻¹)	g_{NU} (cal mol ⁻¹)	$\Delta H_{\text{NU,ZB}}^0 = \Delta H_{\text{vH}}$ (kcal mol ⁻¹)	rel error % ^b
50-peptide	50	0.93	4.0E-03	4.0E-03	326	33.2 (truncated, 10–75 °C)	46.1	0	22.2	444	46.1	
Aspartate receptor fragment	100	1.1	1.0E-03	1.0E-03	327	107.2	103.1	22.7	19.2	192	80.4	3.8
Ubiquitin pH 2.0	70	1.1	2.0E-05		349.3	70.8	70.7	19.8	9.55	136	50.9	0.1
Ubiquitin pH 3.0	70	1.1	2.0E-6		380.4	76.3	76.2	11.0	9.4	134	65.2	0.1
Ubiquitin pH 3.0	76	1.1	3.0E-06		374.3	78.9	79.1	12.0	10.3	136	67.1	-0.3
Apo A1	120	1.1	1.5E-04	6.0E-04	331.1		135.4	50	16.5	138	85.4	2.2
S461L aspartate receptor fragment	110	1.1	1.0E-04	1.0E-04	339.5	64.1	66.2	0	14.6	133	66.2	-3.3
β -lactoglobulin pH 1.1	142	1.1	1.5E-4	1.5E-4	356.3	92.5	98.8	0	17.5	123	98.8	-6.8
β -lactoglobulin pH2.5	142	1.1	5.0E-5		367	96	97.4	0	17.9	126	97.4	1.5
β -lactoglobulin pH 3.3	142	1.1	5.0E-6		372.7	156.5	155.7	67.9	18.1	127	87.8	0.5
S44[A]T4 lysozyme	120	1.1	5.0E-05	5.0E-05	334.5	131.8	126.0	20.4	14.3	119	105.6	4.4
RNase	90	1.1	1.0E-05		332	101.5	103.9	15.5	9.34	104	88.4	-2.4
Lysozyme pH 1.9	129	1.1	2.0E-05		336	143.5	139.9	28.7	11.5	89	103.9	0.1
Ubiquitin (bovine) pH 4.0	76	1.1	1.0E-6		398.3	83.8	84.8	12.1	6.42	84	72.7	-1.2
Ubiquitin pH 4.0	76	1.1	2.0E-6		395	90.2	92.5	10.3	7.7	101	82.2	2.6
Lysozyme pH 2.5	129	1.1	2.0E-06		350	149.5	147.9	20.8	10.4	81	127.1	0.9
Lysozyme pH 2.5	129	1.1	1.0E-06		351	136	134.9	28.4	10.2	79	106.5	0.8
Lysozyme pH 2.5	129	1.1	1.0E-06	1.0E-06	349.5	143.5	139.9	28.3	9.8	76	111.6	2.5
Myoglobin pH 10.7	140	1.1	1.0E-6		364	153.8	157.5	23.82	10.4	74	133.7	
Pseudo WT T4 lysozyme	140	1.1	5.0E-07	5.0E-07	341.2	158.2	157.4	21.7	8.05	59	135.7	0.5

^a Free energy of unfolding calculated with the Zimm–Bragg theory.^b $\Delta H_{\text{exp}}^0 - \Delta H_{\text{calc}}^0 / \Delta H_{\text{exp}}^0$ 

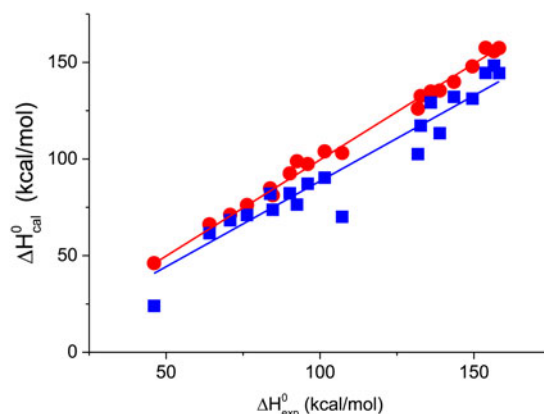


Fig. 10. The calculated unfolding enthalpy is plotted against the experimental result ΔH_{exp}^0 . (●) Zimm–Bragg theory (■) Two-state model).

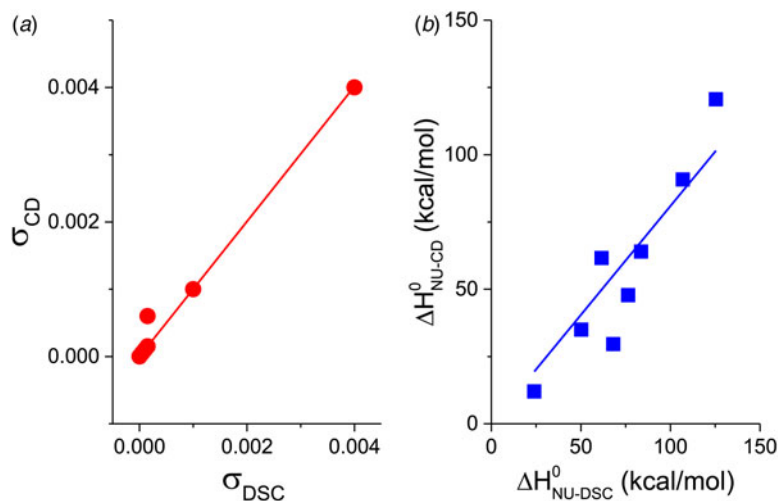


Fig. 11. A comparison of cooperativity parameters deduced from DSC and CD spectroscopy experiments. (a) Zimm–Bragg theory. The nucleation parameter σ_{CD} obtained from CD experiments is plotted against σ_{DSC} , obtained from DSC experiments. A straight line through the origin with slope $m = 1$ is obtained. (b) Two-state model. The conformational enthalpy of the CD experiment, $\Delta H_{\text{NU-CD}}^0$, is plotted against that of the DSC experiment, $\Delta H_{\text{NU-DSC}}^0$.

calorimetric result. This can be traced back, in part, to problems in defining correct baselines in CD spectroscopy. Special algorithms have been proposed to fit ‘sloping baselines’ (Gursky, 2015; Santoro & Bolen, 1988).

The two-state model provides the best agreement between DSC and CD spectroscopy for highly cooperative transitions. Pseudo wild-type T4 lysozyme with its very sharp transition has very similar fit parameters for DSC and CD with $\Delta H_{\text{NU,DSC}}^0 = 125.4 \text{ kcal mol}^{-1}$ and $\Delta H_{\text{NU,CD}}^0 = 120.6 \text{ kcal mol}^{-1}$, respectively.

The two-state model leads to the following conclusions. (i) The conformational enthalpy deduced from CD data, $\Delta H_{\text{NU,CD}}^0$, is typically 20% smaller than that determined by DSC, $\Delta H_{\text{NU,DSC}}^0$. The difference is large for a broad transition and narrows to a few percent for a very cooperative transition. (ii) CD spectroscopy is limited to the so-called conformational enthalpy and cannot detect the change in protein heat capacity, ΔC_p , unless cold-denaturation is measured in the same experiment (Nicholson & Scholtz, 1996; Privalov *et al.* 1986). The heat capacity change upon protein unfolding is an important thermodynamic parameter of the unfolding reaction. It accounts for about 20–50% of the total enthalpy of the unfolding reaction (see Tables 2 and 3).

The unfolding transition of lysozyme was measured with CD spectroscopy (Fig. 5) and DSC (Fig. 8). The fit parameters h , σ , N and T_∞ of the Zimm–Bragg theory were determined from the DSC experiment. Using exactly the same set of parameters a perfect fit of the CD unfolding curve was obtained. A similar result is shown in Fig. 9 for the 50-residue peptide (Scholtz *et al.* 1991a). Again the same set of parameters explains both the DSC and the CD transition. Good agreement between DSC and



CD using the Zimm–Bragg theory was obtained for pseudo wild-type T4 lysozyme (Carra *et al.* 1996), S[44]A T4 lysozyme, (Carra *et al.* 1996) and the aspartate receptor fragment (Wu *et al.* 1995) (cf. Supplementary Information).

6. Zimm–Bragg theory applied to globular proteins

The Zimm–Bragg theory was originally developed for the reversible α -helix-coil transition of synthetic peptides (Zimm & Bragg, 1959). The formalism is however applicable to any linear sequential process with two energetically different states. This suggests that the theory can also be applied to proteins with low α -helix content provided the unfolding is a sequential transition between ‘folded’ and ‘unfolded’ peptide units with enthalpy difference h . As discussed in Section 2.4 ‘hydrophobic and close-packed interactions provide protein stability, while hydrogen bond formation constitutes a structural constraint imposed by the high free energy cost associated with the burying of unsatisfied hydrogen bonding groups’ (Yang & Honig, 1995b). We therefore assume ‘folded’ and ‘unfolded’ peptide units with an enthalpy parameter $h = -1100$ cal mol⁻¹ (except for the 50 amino acid peptide with $h = -930$ cal mol⁻¹).

6.1 Zimm–Bragg theory. An excellent thermodynamic approach to protein unfolding

Table 3 summarizes the parameters of the Zimm–Bragg theory for all proteins investigated. The corresponding simulations of the DSC and CD experiments are shown in Figs 5–8 and in the Supplementary Information. For all DSC unfolding transitions a perfect fit is obtained. The relative error between the experimental enthalpy, ΔH_{exp}^0 , and the Zimm–Bragg calculation, $\Delta H_{\text{calc,ZB}}^0$, is less than 5%.

Table 3 lists the proteins according to increasing cooperativity. The width of the transition, ΔT , is reflected in the nucleation parameter σ . The smaller ΔT , the smaller is the nucleation parameter σ and the sharper and more cooperative is the unfolding process.

The steepness of the transition is determined not only by the nucleation parameter, σ , but also by the number of peptide units, N , participating in the unfolding transition. Only for long chains with $N \gg 1/\sqrt{\sigma}$ is the steepness independent of N and determined exclusively by σ . In contrast, if N is small (as is the case for the 50-amino acid peptide) even very small values of σ cannot generate a steep transition. Proper knowledge of N_{ZB} is hence important for chains, which are shorter than the cooperative length $N_{\text{coop}} = 1/\sqrt{\sigma}$.

The proteins in Table 3 can be divided into three categories. A first group includes proteins with a high helix content and a rather broad transition so that $N \gg 1/\sqrt{\sigma}$ (50-amino acid peptide, Apo A-1, aspartate receptor fragment). The CD spectra of the 50-amino acid peptide (Scholtz *et al.* 1991a) and of recombinant human ApoA-1 (245aa) report an α -helix content of $\sim 98\%$ and $53 \pm 5\%$, respectively, at 20 °C. Upon heating to 90 °C the α -helix content drops to nearly 0% for both molecules. The number of peptide units involved in the unfolding transition is thus $N \approx 50$ and $N \approx 120 \pm 10$, respectively, which is clearly larger than the cooperative chain length. Each helical peptide unit contributes ~ 1.1 kcal mol⁻¹ (50-amino acid peptide: 0.95 kcal mol⁻¹) to the unfolding enthalpy, and the total enthalpies are estimated to be 47.5 kcal mol⁻¹ for the 50-residue peptide and 132 kcal mol⁻¹ for ApoA-1. The experimental enthalpies of 46 and 138.4 kcal mol⁻¹, respectively, are in excellent agreement with these estimates. The aspartate receptor fragment (297aa) is the third member of this group. It is 43% α -helical (~ 114 α -helix peptide units) (Wu *et al.* 1995) and has an enthalpy of unfolding of 107.2 kcal mol⁻¹. It can be estimated that $N = 107.2/1.1 = 97$ amino acid residues participate in the unfolding transition, which is consistent with the change in ellipticity $\epsilon_{222\text{nm}}$ (see Supplementary Information S1).

A second group comprises pseudo-wild type T4 lysozyme (164aa) and its mutant S44[A] lysozyme (165aa) (Carra *et al.* 1996). Both are 61% α -helical according to their ellipticity at 222 nm, corresponding to ~ 100 α -helical peptide units. The total unfolding enthalpies are 158.2 and 131.8 kcal mol⁻¹, respectively, and are clearly larger than the expected ~ 110 kcal mol⁻¹. Additional amino acids residues appear to be involved in the unfolding reaction. Assuming an average unfolding enthalpy of 1.1 kcal mol⁻¹ per peptide unit, 120 peptide units of pseudo WT T4 lysozyme and 140 of S44[A] lysozyme are estimated to participate in unfolding. This allows an excellent fit of the DSC cal mol⁻¹ unfolding curves. A similar analysis can be made for myoglobin, which is about 60% α -helical in solution at 30 °C (Privalov *et al.* 1986) (see Supplementary Information).

The third group comprises proteins with a low α -helix content. Lysozyme (129aa) has at most 30 α -helical peptide units. The α -helix content of ubiquitin (79aa) (Ibarra-Molero *et al.* 1999a) and RNase (129aa) (Kurapkat *et al.* 1997) can be estimated to be less than 30%. Nevertheless the unfolding enthalpies of these three enzymes are large. We again assume a sequential unfolding with an average enthalpy of 1.1 kcal mol⁻¹ per peptide unit. Consequently, ~ 120 peptide units are estimated to



become unfolded in lysozyme, ~70 in ubiquitin, and ~90 in RNase. With these numbers the Zimm–Bragg theory provides a perfect fit of the DSC data of the three proteins.

6.2 The free energy change upon thermal and chemical denaturation

Table 1 lists the width of the unfolding transition, ΔT , for the different proteins investigated. The change of the Gibbs free energy in this temperature interval is the free energy of unfolding ΔG_{NU}^0 . It can be calculated with either the two-state model (Eq. (17)) or the Zimm–Bragg theory (Eq. (22)). Tables 2 and 3 summarise the corresponding ΔG_{NU}^0 -values. The two-state model predicts numerical values between 5 and 10 kcal mol⁻¹. The variability is larger for the Zimm–Bragg theory with ΔG_{NU}^0 in the range of 6 kcal mol⁻¹ \leq ΔG_{NU}^0 \leq 22 kcal mol⁻¹.

The Gibbs free energy per peptide unit, $g_{\text{NU}} = \Delta G_{\text{NU}}^0/n$, calculated with the Zimm–Bragg theory, is linearly correlated with the width of the transition ΔT (g_{NU} (cal mol⁻¹) = 3·17 ΔT + 3·9; Supplementary Information S18). It changes from $g_{\text{NU}} = 440$ cal mol⁻¹ for the broad transition of the 50-amino acid peptide to $g_{\text{NU}} = 57$ cal mol⁻¹ for the highly cooperative transition of pseudo WT T4 lysozyme. In contrast, no systematic variation of ΔG_{NU}^0 can be recognized for the two-state model.

Thermal protein unfolding can be compared with chemical denaturation. In this protocol, the fraction of unfolded protein is measured with spectroscopic techniques at different concentrations of denaturant. The equilibrium constant K_{NU} and the corresponding free energy ΔG_{NU} are calculated with the two-state model. ΔG_{NU} is then plotted as a function of denaturant concentration and extrapolated to zero denaturant concentration (linear extrapolation method, LEM) (Bolen & Yang, 2000; Konermann, 2012) The free energy at zero denaturant concentration is assumed to be equivalent to the free energy change produced by heat denaturation. Chemical denaturation is however a multi-site equilibrium and not a two-state process. The denaturants (guanidineHCl, urea) bind to a large number of units by electrostatic and/or hydrophobic forces (Makhatadze & Privalov, 1992). It has been noted: ‘Given that ΔG_{NU}^0 values are often determined from a method that is empirical in origin (the linear extrapolation method) it is doubtful that the quantity we call ΔG_{NU}^0 deserves the complete credibility it is often given’ (Bolen & Yang, 2000).

The thermal denaturation of lysozyme under conditions described in Figs 6 and 8 occurs between 50 and 73 °C. The free energy of unfolding is $\Delta G_{\text{NU}}^0 = 6.3$ kcal mol⁻¹, calculated with the two-state model and the CD-parameter $\Delta H_{\text{NU}}^0 = 90.8$ kcal mol⁻¹. Using the DSC parameters $\Delta H_{\text{NU}}^0 = 106.9$ kcal mol⁻¹ and $\Delta C_{\text{p,NU}}^0 = 2.269$ kcal molK⁻¹ results in $\Delta G_{\text{NU}}^0 = 7.3$ kcal mol⁻¹. The Zimm–Bragg theory predicts $\Delta G_{\text{NU}}^0 = 9.8$ kcal mol⁻¹ based on the DSC experiment. Chemical denaturation experiments at 20 °C with guanidine HCl resulted in $\Delta G_{\text{NU}}^0 = 8.9$ kcal mol⁻¹ (pH 7.0) (Ahmad *et al.* 1982) and 8.2 kcal mol⁻¹ (pH 6.0) (Laurents & Baldwin, 1997).

The Zimm–Bragg theory can easily be modified to describe chemical denaturation. This is explained briefly in Supplementary Information S19.

7. Conclusions

The two-state model treats protein unfolding as a single global event. The Zimm–Bragg theory, in contrast, sees it as a sequence of local processes. Thermally-induced protein unfolding is a sequential multi-state process. Even if intermediate states are only sparsely populated a sequential model is physically more realistic than a two-state model.

The Zimm–Bragg theory predicts a sequential unfolding and accounts for intermediate states. A ‘folded’ \rightleftharpoons ‘unfolded’ equilibrium of peptide units with an average unfolding enthalpy of 1.1 kcal mol⁻¹ is valid also for proteins with low α -helix content. The Zimm–Bragg theory provides a perfect fit to the DSC data of all proteins investigated and describes equally well the CD transition curves with the same parameters. It predicts the calorimetric heat of unfolding, ΔH_{exp}^0 , with an error of less than 5%. In contrast, the two-state model requires different parameters for DSC- and CD- unfolding transitions. The calculated unfolding enthalpy $\Delta H_{\text{calc,2-state}}^0$ is typically 10–20% smaller than the experimental result ΔH_{exp}^0 . Moreover, the enthalpies determined from CD spectroscopy data are even smaller than those accused is the two-state model from DSC experiments.

The observation of an isodichroic point is not sufficient evidence for an equilibrium between just two unique protein conformations (‘native’ and ‘unfolded’). An isodichroic point can also be generated by an *intramolecular* equilibrium between ‘folded’ and ‘unfolded’ peptide units. The solution can thus contain a manifold of protein conformations, each protein containing a different fraction of “folded” and “unfolded” peptide units.

Supplementary material

The supplementary material for this article can be found at <http://dx.doi.org/10.1017/S0033583516000044>.



Acknowledgements

We are indebted to T. Schulthess for measuring the CD and DSC transitions of Apo A-1. We are grateful to X. Li-Blatter for the CD and DSC measurements of lysozyme.

References

- AHMAD, F. & BIGELOW, C. C. (1982). Estimation of the free energy of stabilization of ribonuclease A, lysozyme, alpha-lactalbumin, and myoglobin. *The Journal of Biological Chemistry* **257**, 12935–12938.
- ARNULPHI, C., JIN, L. H., TRICERRI, M. A. & JONAS, A. (2004). Enthalpy-driven apolipoprotein A-I and lipid bilayer interaction indicating protein penetration upon lipid binding. *Biochemistry* **43**, 12258–12264.
- BOLEN, D. W. & YANG, M. (2000). Effects of guanidine hydrochloride on the proton inventory of proteins: implications on interpretations of protein stability. *Biochemistry* **39**, 15208–15216.
- CARRA, J. H., MURPHY, E. C. & PRIVALOV, P. L. (1996). Thermodynamic effects of mutations on the denaturation of T4 lysozyme. *Biophysical Journal* **71**, 1994–2001.
- CHOU, P. Y. & SCHERAGA, H. A. (1971). Calorimetric measurement of enthalpy change in isothermal helix-coil transition of poly-L-lysine in aqueous solution. *Biopolymers* **10**, 657–680.
- DAVIDSON, N. (1962). In *Statistical Mechanics*, p. 385. New York: Mac Graw-Hill.
- DELBAERE, L. T., VANDONSELAAR, M., PRASAD, L., QUAIL, J. W., WILSON, K. S. & DAUTER, Z. (1993). Structures of the lectin IV of Griffonia simplicifolia and its complex with the Lewis b human blood group determinant at 2.0 Å resolution. *Journal of Molecular Biology* **230**, 950–965.
- DOIG, A. J. (2002). Recent advances in helix-coil theory. *Biophysical Chemistry* **101–102**, 281–293.
- FERNANDEZ-VIDALL, M., JAYASINGHE, S., LADOKHIN, A. S. & WHITE, S. H. (2007). Folding amphipathic helices into membranes: amphiphilicity trumps hydrophobicity. *Journal of Molecular Biology* **370**, 459–470.
- FREIRE, E. & MURPHY, K. P. (1991). Molecular-basis of cooperativity in protein folding. *Journal of Molecular Biology* **222**, 687–698.
- GARCIA-HERNANDEZ, E., HERNANDEZ-ARANA, A., ZUBILLAGA, R. A. & ROJO-DOMINGUEZ, A. (1998). Spectroscopic and thermodynamic evidence for a complex denaturation mechanism of bovine beta-lactoglobulin A. *Biochemistry and Molecular Biology International* **45**, 761–768.
- GURSKY, O. (2015). Structural stability and functional remodeling of high-density lipoproteins. *Febs Letters* **589**, 2627–2639.
- GURSKY, O. & ATKINSON, D. (1996). Thermal unfolding of human high-density apolipoprotein A-1: implications for a lipid-free molten globular state. *Proceedings of the National Academy of Sciences of the United States of America* **93**, 2991–2995.
- IBARRA-MOLERO, B., LOLADZE, V. V., MAKHATADZE, G. I. & SANCHEZ-RUIZ, J. M. (1999a). Thermal versus guanidine-induced unfolding of ubiquitin. An analysis in terms of the contributions from charge-charge interactions to protein stability. *Biochemistry* **38**, 8138–8149.
- IBARRA-MOLERO, B., MAKHATADZE, G. I. & SANCHEZ-RUIZ, J. M. (1999b). Cold denaturation of ubiquitin. *Biochimica et biophysica acta* **1429**, 384–390.
- JIA, Z., QUAIL, J. W., WAYGOOD, E. B. & DELBAERE, L. T. (1993). The 2.0-Å resolution structure of *Escherichia coli* histidine-containing phosphocarrier protein HPr. A redetermination. *The Journal of Biological Chemistry* **268**, 22490–22501.
- KIEFHABER, T. (1995). Kinetic traps in lysozyme folding. *Proceedings of the National Academy of Sciences of the United States of America* **92**, 9029–9033.
- KONERMANN, L. (2012). *Protein Unfolding and Denaturants*. Chichester: eLSJohn Wiley & Sons, Ltd, pp. 1–7.
- KURAPKAT, G., KRUGER, P., WOLLMER, A., FLEISCHHAUER, J., KRAMER, B., ZOBEL, E., KOSLOWSKI, A., BOTTERWECK, H. & WOODY, R. W. (1997). Calculations of the CD spectrum of bovine pancreatic ribonuclease. *Biopolymers* **41**, 267–287.
- LAURENTS, D. V. & BALDWIN, R. L. (1997). Characterization of the unfolding pathway of hen egg white lysozyme. *Biochemistry* **36**, 1496–1504.
- LI, Y., HAN, X. & TAMM, L. K. (2003). Thermodynamics of fusion peptide-membrane interactions. *Biochemistry* **42**, 7245–7251.
- LUO, P. & BALDWIN, R. L. (1997). Mechanism of helix induction by trifluoroethanol: a framework for extrapolating the helix-forming properties of peptides from trifluoroethanol/water mixtures back to water. *Biochemistry* **36**, 8413–8421.
- MAKHATADZE, G. I. & PRIVALOV, P. L. (1992). Protein interactions with urea and guanidinium chloride. A calorimetric study. *Journal of Molecular Biology* **226**, 491–505.
- MARQUSEE, S., ROBBINS, V. H. & BALDWIN, R. L. (1989). Unusually stable helix formation in short alanine-based peptides. *Proceedings of the National Academy of Sciences of the United States of America* **86**, 5286–5290.
- MEI, X. & ATKINSON, D. (2011). Crystal structure of C-terminal truncated apolipoprotein A-I reveals the assembly of high density lipoprotein (HDL) by dimerization. *The Journal of Biological Chemistry* **286**, 38570–38582.
- MEIER, M. & SEELIG, J. (2007). Thermodynamics of the coil \rightleftharpoons beta-sheet transition in a membrane environment. *Journal of Molecular Biology* **369**, 277–289.
- MEIER, M. & SEELIG, J. (2008). Length dependence of the coil \rightleftharpoons beta-sheet transition in a membrane environment. *Journal of the American Chemical Society* **130**, 1017–1024.
- MIRANKER, A., RADFORD, S. E., KARPLUS, M. & DOBSON, C. M. (1991). Demonstration by NMR of folding domains in lysozyme. *Nature* **349**, 633–636.
- MORRISSET, J. D., DAVID, J. S. K., POWNALL, H. J. & GOTTO, A. M. (1973). Interaction of an apolipoprotein (Apolp-Alanine) with phosphatidylcholine. *Biochemistry* **12**, 1290–1299.



- MYERS, J. K., PACE, C. N. & SCHOLTZ, J. M. (1995). Denaturant m values and heat capacity changes: relation to changes in accessible surface areas of protein unfolding. *Protein Science: a Publication of the Protein Society* **4**, 2138–2148.
- NICHOLSON, E. M. & SCHOLTZ, J. M. (1996). Conformational stability of the *Escherichia coli* HPr protein: test of the linear extrapolation method and a thermodynamic characterization of cold denaturation. *Biochemistry* **35**, 11369–11378.
- PRIVALOV, G., KAVINA, V., FREIRE, E. & PRIVALOV, P. L. (1995). Precise scanning calorimeter for studying thermal-properties of biological macromolecules in dilute-solution. *Analytical Biochemistry* **232**, 79–85.
- PRIVALOV, P. L. (1997). Thermodynamics of protein folding. *Journal of Chemical Thermodynamics* **29**, 447–474.
- PRIVALOV, P. L. & DRAGAN, A. I. (2007). Microcalorimetry of biological macromolecules. *Biophysical Chemistry* **126**, 16–24.
- PRIVALOV, P. L. & GILL, S. J. (1988). Stability of protein-structure and hydrophobic interaction. *Advances in Protein Chemistry* **39**, 191–234.
- PRIVALOV, P. L., GRIKO, Y. V., VENYAMINOV, S. Y. & KUTYSHENKO, V. P. (1986). Cold denaturation of myoglobin. *Journal of Molecular Biology* **190**, 487–498.
- PRIVALOV, P. L. & MAKHATADZE, G. I. (1990). Heat-capacity of proteins.2. Partial molar heat-capacity of the unfolded polypeptide-chain of proteins – protein unfolding effects. *Journal of Molecular Biology* **213**, 385–391.
- PRIVALOV, P. L. & MAKHATADZE, G. I. (1993). Contribution of hydration to protein folding thermodynamics. II. The entropy and Gibbs energy of hydration. *Journal of Molecular Biology* **232**, 660–679.
- PRIVALOV, P. L., TIKTOPULO, E. I., VENYAMINOV, S. Y., GRIKO, Y. V., MAKHATADZE, G. I. & KHECHINASHVILI, N. N. (1989). Heat-capacity and conformation of proteins in the denatured state. *Journal of Molecular Biology* **205**, 737–750.
- RADFORD, S. E., DOBSON, C. M. & EVANS, P. A. (1992). The folding of hen lysozyme involves partially structured intermediates and multiple pathways. *Nature* **358**, 302–307.
- REED, J. & REED, T. A. (1997). A set of constructed type spectra for the practical estimation of peptide secondary structure from circular dichroism. *Analytical Biochemistry* **254**, 36–40.
- RIALDI, G. & HERMANS, J. (1966). Calorimetric heat of helix-coil transition of poly-L-glutamic acid. *Journal of the American Chemical Society* **88**, 5719–5720.
- ROSGEN, J. & HINZ, H. J. (2000). Response functions of proteins. *Biophysical Chemistry* **83**, 61–71.
- SAITO, H., DHANASEKARAN, P., NGUYEN, D., DERIDDER, E., HOLVOET, P., LUND-KATZ, S. & PHILLIPS, M. C. (2004). Alpha-Helix formation is required for high affinity binding of human apolipoprotein A-I to lipids. *Journal of Biological Chemistry* **279**, 20974–20981.
- SAITO, H., DHANASEKARAN, P., NGUYEN, D., HOLVOET, P., LUND-KATZ, S. & PHILLIPS, M. C. (2003a). Domain structure and lipid interaction in human apolipoproteins A-I and E, a general model. *Journal of Biological Chemistry* **278**, 23227–23232.
- SAITO, H., LUND-KATZ, S. & PHILLIPS, M. C. (2003b). Domain structure and lipid interaction in human apolipoprotein A-I. *Atherosclerosis Supplements* **4**, 221–221.
- SANTORO, M. M. & BOLEN, D. W. (1988). Unfolding free energy changes determined by the linear extrapolation method. 1. Unfolding of phenylmethanesulfonyl alpha-chymotrypsin using different denaturants. *Biochemistry* **27**, 8063–8068.
- SCHOLTZ, J. M. (1991). Correction. *Proceedings of the National Academy of Sciences of the United States of America* **88**, 6898–6898.
- SCHOLTZ, J. M., MARQUESE, S., BALDWIN, R. L., YORK, E. J., STEWART, J. M., SANTORO, M. & BOLEN, D. W. (1991a). Calorimetric determination of the enthalpy change for the alpha-helix to coil transition of an alanine peptide in water. *Proceedings of the National Academy of Sciences of the United States of America* **88**, 2854–2858.
- SCHOLTZ, J. M., QIAN, H., YORK, E. J., STEWART, J. M. & BALDWIN, R. L. (1991b). Parameters of helix-coil transition theory for alanine-based peptides of varying chain lengths in water. *Biopolymers* **31**, 1463–1470.
- SCHULTHESS, T., SCHÖNFELD, H. J. & SEELIG, J. (2015). Thermal unfolding of apolipoprotein A-I. Evaluation of methods and models. *Biochemistry* **54**, 3063–3075.
- SCHWARZ, F. P. (1990). Biological thermodynamic data for the calibration of differential scanning calorimeters – heat-capacity data on the unfolding transition of beta-lactoglobulin in solution. *Thermochimica Acta* **159**, 305–325.
- SEELEY, S. K., WITTROCK, G. K., THOMPSON, L. K. & WEIS, R. M. (1996). Oligomers of the cytoplasmic fragment from the *Escherichia coli* aspartate receptor dissociate through an unfolded transition state. *Biochemistry* **35**, 16336–16345.
- SUURKUUSK, M. & HALLEN, D. (1999). Denaturation of apolipoprotein A-I and the monomer form of apolipoprotein A-I-Milano. *European Journal of Biochemistry* **265**, 346–352.
- TALL, A. R., SHIPLEY, G. G. & SMALL, D. M. (1976). Conformational and thermodynamic properties of apo A-I of human plasma high density lipoproteins. *Journal of Biological Chemistry* **251**, 3749–3755.
- TALL, A. R., SMALL, D. M., SHIPLEY, G. G. & LEES, R. S. (1975). Apoprotein stability and lipid-protein interactions in human plasma high density lipoproteins. *Proceedings of the National Academy of Sciences of the United States of America* **72**, 4940–4942.
- TANAKA, M., KOYAMA, M., DHANASEKARAN, P., NGUYEN, D., NICKEL, M., LUND-KATZ, S., SAITO, H. & PHILLIPS, M. C. (2008). Influence of tertiary structure domain properties on the functionality of apolipoprotein A-I. *Biochemistry* **47**, 2172–2180.
- WIEPRECHT, T., APOSTOLOV, O., BEYERMANN, M. & SEELIG, J. (1999). Thermodynamics of the alpha-helix-coil transition of amphipathic peptides in a membrane environment: implications for the peptide-membrane binding equilibrium. *Journal of Molecular Biology* **294**, 785–794.
- WIEPRECHT, T., APOSTOLOV, O. & SEELIG, J. (2000). Binding of the antibacterial peptide magainin 2 amide to small and large unilamellar vesicles. *Biophysical Chemistry* **85**, 187–198.
- WU, J. R., LONG, D. G. & WEIS, R. M. (1995). Reversible dissociation and unfolding of the *Escherichia-coli* aspartate receptor cytoplasmic fragment. *Biochemistry* **34**, 3056–3065.



- YANG, A. S. & HONIG, B. (1995a). Free-energy determinants of secondary structure formation .2. Antiparallel beta-sheets. *Journal of Molecular Biology* **252**, 366–376.
- YANG, A. S. & HONIG, B. (1995b). Free energy determinants of secondary structure formation: I. alpha-Helices. *Journal of Molecular Biology* **252**, 351–365.
- ZEHENDER, F., ZIEGLER, A., SCHÖNFELD, H. J. & SEELIG, J. (2012). Thermodynamics of protein self-association and unfolding. The case of apolipoprotein A-I. *Biochemistry* **51**, 1269–1280.
- ZHOU, Y., HALL, C. K. & KARPLUS, M. (1999). The calorimetric criterion for a two-state process revisited. *Protein Science: a Publication of the Protein Society* **8**, 1064–1074.
- ZIMM, B. H. & BRAGG, J. K. (1959). Theory of the phase transition between helix and random coil in polypeptide chains. *Journal of Chemical Physics* **31**, 526–535.